PERGAMON

Journal of Structural Geology 24 (2002) 219–239

JOURNAL OF STRUCTURAL GEOLOGY

www.elsevier.com/locate/jstrugeo

Kinematics of oblique collision and ramping inferred from microstructures and strain in middle crustal rocks, central Southern Alps, New Zealand ☆

T.A. Little[a,*], R.J. Holcombe[b], B.R. Ilg[a]

[a]*School of Earth Sciences; Victoria University of Wellington; P.O. Box 600, Wellington, New Zealand*
[b]*Department of Earth Sciences, University of Queensland, Queensland, 4072, Australia*

Received 12 June 2000; revised 5 April 2001; accepted 23 April 2001

Abstract

The hanging wall of the Alpine Fault near Franz Josef Glacier has been exhumed during the past ~2–3 m.y. providing a sample of the ductilely deformed middle crust of a modern obliquely convergent orogen. Presently exposed rocks of the Pacific Plate are inferred to have undergone several phases of ductile deformation as they moved westward above a mid-crustal detachment. Initially they were transpressed across the outboard part of the orogen, resulting in oblate fabrics with a down-dip stretch. Later, they encountered the Alpine Fault, experiencing an oblique-slip backshearing on vertical planes. This escalator-like deformation tilted and thinned the incoming crust onto that crustal-scale oblique ramp. This style of hanging wall deformation may affect only the most rapidly uplifting, central part of the Southern Alps because of the low flexural rigidity of the crust in that region and its displacement over a relatively sharp ramp-angle at depth. A 3D transpressive flow affected mylonites locally near the fault, but their shear direction remained parallel to plate motion, ruling out ductile 'extrusion' as an important process in this orogen. Outside the mylonite zone, late Cenozoic shortening is inferred to be modest (30–40%), as measured from deformation of younger biotite grains. Oblique collision is dominated by translation on the Alpine Fault, and rocks migrate rapidly through the deforming zone, preventing the accumulation of large finite strains. Transpression may play a minor role in oblique collision.

Keywords: Oblique collision; Ramping; Alpine Fault; Transpression

1. Introduction

The central part of the Southern Alps in New Zealand is an ~150-km-wide zone of active oblique plate convergence in continental crust (Norris et al., 1990). Vigorous erosion along the western side of this orogen, together with marked contrasts in thermal structure and crustal strength cause deformation to be focused into a narrow zone along the Alpine Fault (Fig. 1) (Koons, 1987, 1990; Norris and Cooper, 1997). Oblique-reverse slip on this fault has resulted in rapid uplift and erosion of Pacific Plate rocks on its hanging wall (Sibson et al., 1981). During the past ~3–5 m.y. rocks to the east of the fault have been exhumed from depths of 20–30 km (e.g. Grapes, 1995) to expose ductile fabrics that were developed at deep levels of this active transpressive orogen. The plate kinematics of the Southern Alps are well constrained from sea-floor spreading and geodetic data (Walcott, 1998; Beavan et al., 1999), and its deep structure has recently been imaged geophysically (Davey et al., 1998; Molnar et al., 1999). Tectonite fabrics in the hanging wall of the Alpine Fault thus occur in a well-understood geodynamical context and provide a rare opportunity to infer processes and mechanisms of oblique continental convergence from observations of naturally deformed rocks.

Zones of oblique convergence have been the subject of extensive geodynamical and strain modelling. In many studies the Southern Alps are cited as an example of a plate margin across which oblique motion components are not strongly partitioned into separate parallel zones of strike-slip and convergent deformation (e.g. Koons, 1994; Braun and Beaumont, 1995; Teyssier et al., 1995; Beaumont et al., 1996; Jiang et al. 2001). An extensive literature has also developed on the theory of transpression and the progressive development of strain and deformational fabrics in such zones (e.g. Sanderson and Marchini, 1984; Tikoff and Fossen, 1993, 1999; Dutton, 1997; Holdsworth et al., 1998; Jiang and Williams, 1998, Passchier, 1998).

☆ See "Electronic Supplements" on this journal's homepage: http://www.elsevier.com/locate/jstrugeo

* Corresponding author. Tel.: +64-4-463-5233-8404; fax: +64-4-463-5186.

E-mail address: timothy.little@vuw.ac.nz (T.A. Little).

0191-8141/02/$ - see front matter
PII: S0191-8141(01)00060-8

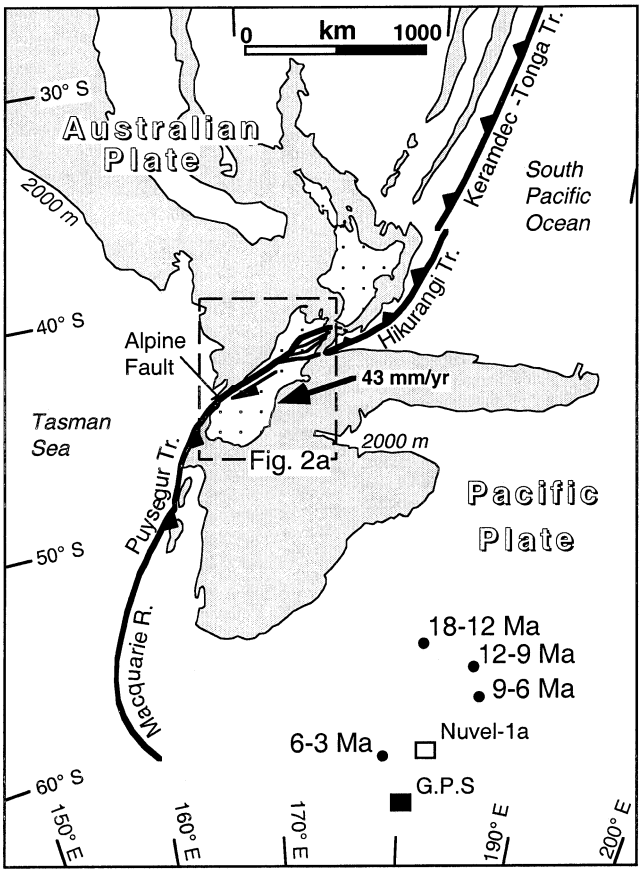

Fig. 1. Index map of Pacific–Australian plate boundary in New Zealand showing location of Alpine Fault and selected stage poles and instantaneous (G.P.S.-derived) pole for Pacific–Australia plate motion since 18 Ma (black circles), after Walcott (1998). Estimates of the contemporary Euler pole includes a recent G.P.S.-derived estimate (black square) and the <3 Ma estimate of Nuvel-1a (DeMets et al., 1994) (white square).

Transpression can be defined as a combination of strike-slip shear and irrotational strain across a tabular zone that is thinned by the deformation, and is a concept that refers to 3D patterns of instantaneous flow. 'Oblique convergence', however, refers to relative plate motions in a horizontal reference frame (e.g. Dewey et al., 1998). Despite the global importance of both types of zones (e.g. Woodcock, 1986), field studies of natural examples within a well-constrained kinematic context are rare.

Existing work in the central part of the Southern Alps has led to conflicting interpretations about the role of transpressive deformation to the east of the Alpine Fault in accommodating oblique convergence between the Pacific and Australian plates. Sibson et al. (1979) measured stretching lineations in the Alpine mylonite zone bordering the Alpine Fault, arguing that oblique simple shear along the Alpine Fault at depth translates its hanging wall parallel to the plate motion vector. Fault-surface lineations in gouge and cataclasite along the Alpine Fault support this interpretation (Cooper and Norris, 1994; Norris and Cooper, 1995, 1997). Walcott (1998) used the steep plunge of some of Sibson et al.'s stretching lineations to infer that the shear direction in the Alpine mylonites deviates clockwise from the plate motion. He attributed this discordance to tectonic extrusion of a ~5-km-wide panel of schists to the east of both the Alpine Fault and its mylonite zone, presumably a type of transpression, which increases the dip-parallel velocity of rocks attached to the western side of that panel. Jiang et al. (2001) used the same data set, in particular the variable to steep plunge of the lineations, to argue for transpressive shear in the ~1-km-wide mylonite zone, a deformation that includes dip-parallel stretching of the Alpine Fault.

Our chief goal here will be to understand how oblique motion between the Pacific and Australian plates has been accommodated during the past ~6 m.y and the role of transpressive flow in taking up that oblique convergence. Central to this issue is the degree to which deformation is partitioned between slip on the Alpine Fault and its mylonite zone, on the one hand, and distributed deformation of its hanging wall rocks on the other. Late Quaternary slip rates on the Alpine Fault suggest that most of the plate motion in the central part of the South Island is taken up by slip on that fault (e.g. Cooper and Norris, 1994; Sutherland and Norris, 1995). As the Australian Plate rocks to the west are relatively undeforming (Beavan et al., 1999), the remaining plate motion must be distributed across the ~150 km width of the Southern Alps to the east, a region of active strike-slip and reverse-slip faulting on the surface (Norris et al., 1990). G.P.S. geodetic data across the central Southern Alps confirm that oblique crustal shortening is distributed across the ~150 km width of the orogen, and an elastic-dislocation model implies that ~40–50% of the plate motion is taken up in deformation to the east of the Alpine Fault (Beavan et al., 1999).

In this paper we will examine structural field data from deeply exhumed parts of the Pacific Plate in a central part of the Southern Alps. Several measures of strain in biotite and garnet-zone schists will be used to describe aspects of finite and incremental strain in the non-mylonitic part of the Alpine Fault's hanging wall. Although the deformational fabrics are complicated by inherited elements, we will attempt to isolate the youngest, late Cenozoic strain increment. Our data will be used to address questions of the following types. What structures develop during oblique collision of middle crustal rocks in the Southern Alps, and how much strain do they accommodate? What processes accommodate crustal-scale ramping of Pacific Plate rocks onto the oblique ramp of the Alpine Fault? What role, if any, does transpressive flow or tectonic extrusion play in accommodating oblique convergence in the Southern Alps and where does it take place? Is transpression monoclinic or triclinic in symmetry, and does it seem to accumulate as a steady-state flow or in a series of non-coaxial steps? Our new data will be synthesized with recent geophysical data to develop a preliminary kinematic model for how middle

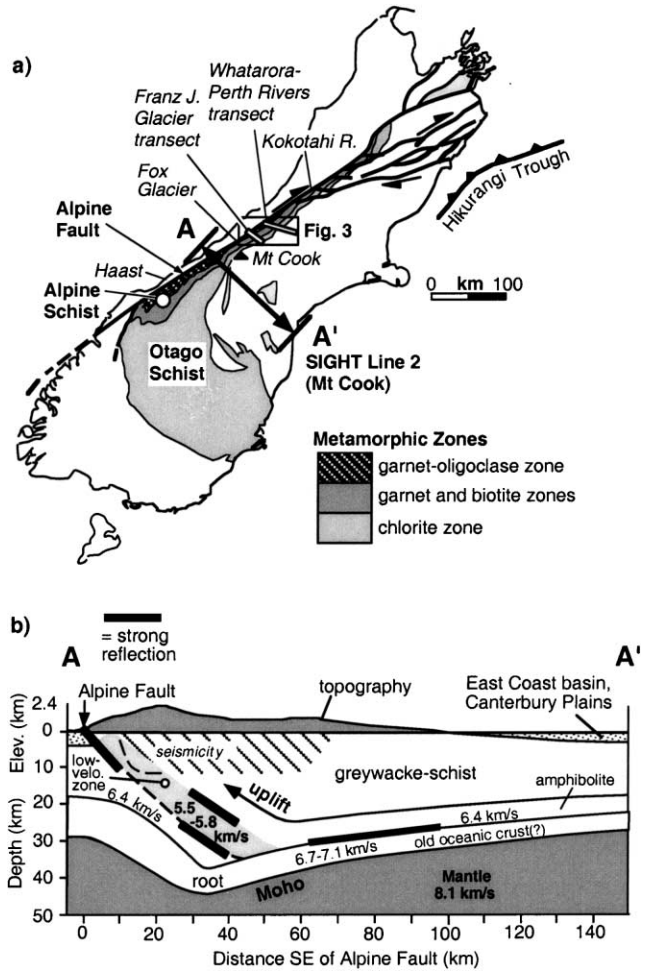

Fig. 2. (a) Tectonic and metamorphic map of South Island showing location of the two structural transects. Cross-section A–A′ is the onshore part of a recently acquired deep crustal seismic transect near Mt. Cook (line 2 of the SIGHT project). (b) Preliminary interpretation of crustal structure of onland part of SIGHT seismic transect (line 2) across the central South Island, New Zealand (from Davey et al., 1998; Kleffman et al., 1998; Stern et al., 2001).

crustal rocks respond to oblique collision in a central part of the Southern Alps.

The field data were collected on two valley transects across the central part of the Southern Alps near Franz Josef Glacier and Whataroa River, with additional data being collected in streams between Franz Josef and Fox Glaciers (Fig. 2a). We examined outcrop-scale structures as well as microstructures in >200 oriented samples. Most of these were cut into at least two mutually orthogonal thin-sections, perpendicular to foliation (Little et al., 2002). Whereas the sequence, spatial distribution, structural geometry, and shear sense of ductile fabrics occurring in the SE-tilted crustal section of Pacific Plate rocks was detailed in Little et al. (2002), our focus here is in on the youngest ductile fabrics and the implication of their strain state, measured by several different techniques, for the kinematics of oblique collision and crustal-scale ramping in the Southern Alps.

2. Plate tectonic setting

The Alpine Fault was established as a dextral transform structure between the Australian and Pacific Plates by ~25 Ma (e.g. Cooper et al., 1987; Sutherland, 1995). At ~6.4 Ma, a marked increase in the plate convergence component resulted in uplift of the Southern Alps (Walcott, 1998) (Fig. 1). Since then, ~90 km of plate convergence and ~230 km of strike-slip has been accommodated across the central part of the range (Walcott, 1998). Recent G.P.S data indicate that the Pacific Plate in that region moves WSW relative to the Australian Plate, about ~22° clockwise of the strike of the Alpine Fault (Larson et al., 1997). This vector resolves into ~40 mm/year of slip parallel to that structure and ~16 mm/year of convergence. Based on offset landfoms, the Alpine Fault has a late Quaternary strike-slip rate of 25–30 mm/year, and accommodates about 55–80% of the total plate motion (Cooper and Norris, 1994; Sutherland, 1995; Sutherland and Norris, 1995). Near the surface, the central section of the Alpine Fault is segmented into NNE-striking oblique-thrust sections and ENE-striking, vertical strike-slip sections, whereas at depth it is probably a single dextral-reverse structure that dips SE at 50° (Norris and Cooper, 1995). In the central Southern Alps, rates of rock uplift to the east of the Alpine Fault are estimated at ~5–12 mm/year (Bull and Cooper, 1986; Simpson et al., 1994; Walcott, 1998).

Today, the Pacific Plate is believed to be delaminating along a subhorizontal interface at depths of 20–30 km, with rocks above this decollement being uplifted and exhumed along the Alpine Fault ramp, and rocks below it being underthrust or thickened in some way (Wellman, 1979; Norris et al., 1990; Molnar et al., 1999). A recent seismic profile near Mt Cook has imaged a moderately dipping Alpine Fault shallowing downward towards an apparent decollement level at ~30 km (Kleffman et al., 1998; Stern et al., 2001) (Fig. 2b). Beneath this decollement, a crustal root extends down to a depth of ~40–45 km (Davey et al., 1998). Above it, magnetotelluric and P-wave velocity anomalies suggest that the Alpine Fault is mantled by a conductive zone containing overpressured metamorphic fluids (Wannamaker et al., 2001; Stern et al., 2001). Rapid uplift and erosion causes the modern brittle-ductile transition to the east of the Alpine Fault to be shallow, perhaps only ~8–10 km deep (Koons, 1987; Craw, 1997).

Directions of maximum geodetic shortening rate in the west-central part of the Southern Alps, including those derived recently from G.P.S. data, typically trend ~110–120° (Fig. 3) (Walcott, 1979; Pearson et al., 1995; Beavan et al., 1999). As Holm et al. (1989) pointed out, this shortening direction is approximately perpendicular to a near-vertical foliation in the non-mylonitic part of the Alpine Schist (Fig. 3).

3. Ductile fabrics in the Alpine Schist

The uplifted, eastern side of the Alpine Fault embraces a

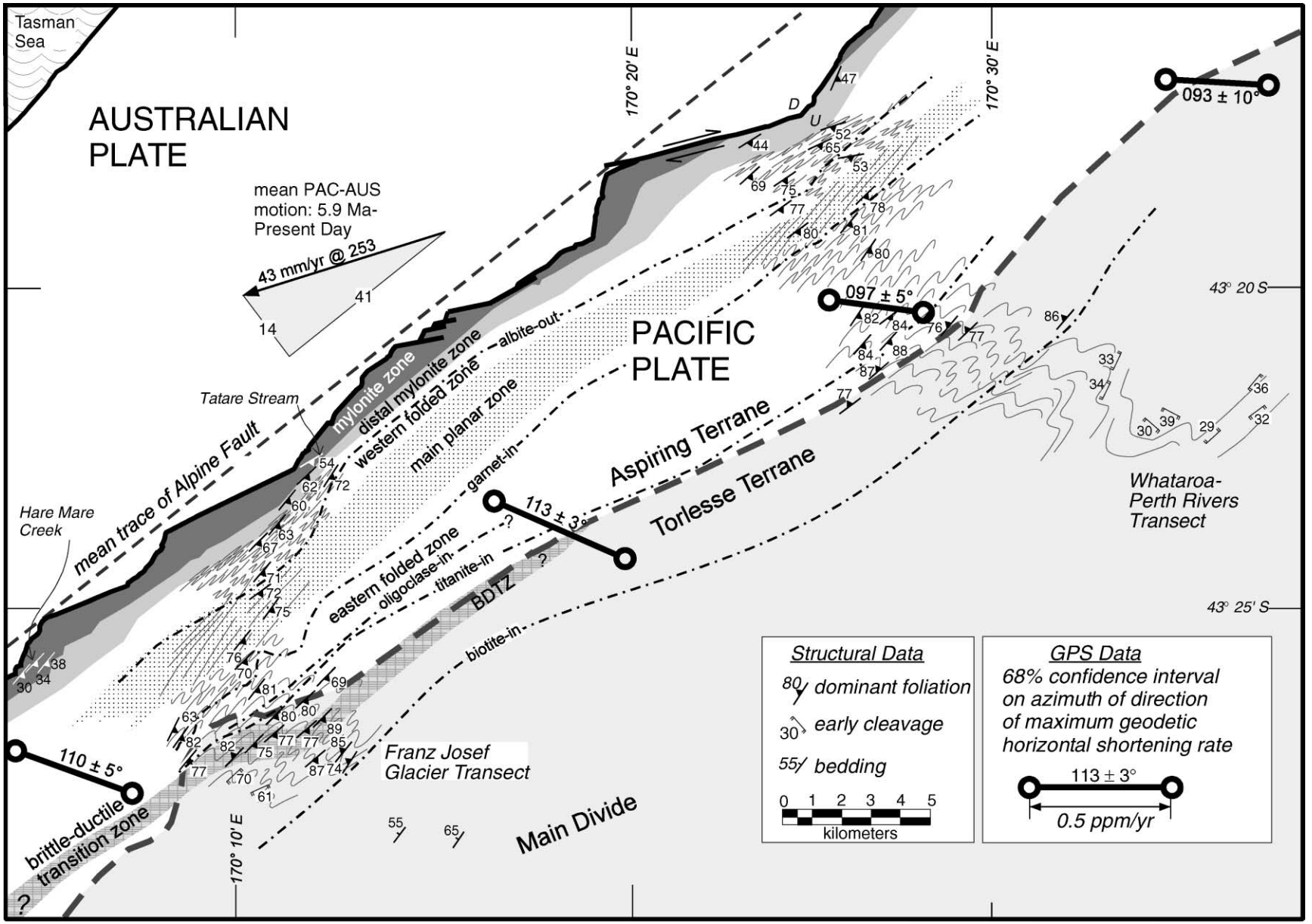

Fig. 3. Simplified geological map of a central part of the Southern Alps, near Franz Josef Glacier, showing the Alpine Fault, tectonic units and isograds in the Alpine Schist, selected structural data, and geodetic directions of maximum horizontal shortening rate (from Beavan et al., 1999). See Fig. 2a for location. Also shown is post-5.9 Ma average Pacific–Australian plate motion vector near Franz Josef Glacier (43 mm/year) using the rotation parameters of Walcott (1998). Alpine Fault trace is from Norris and Cooper (1995).

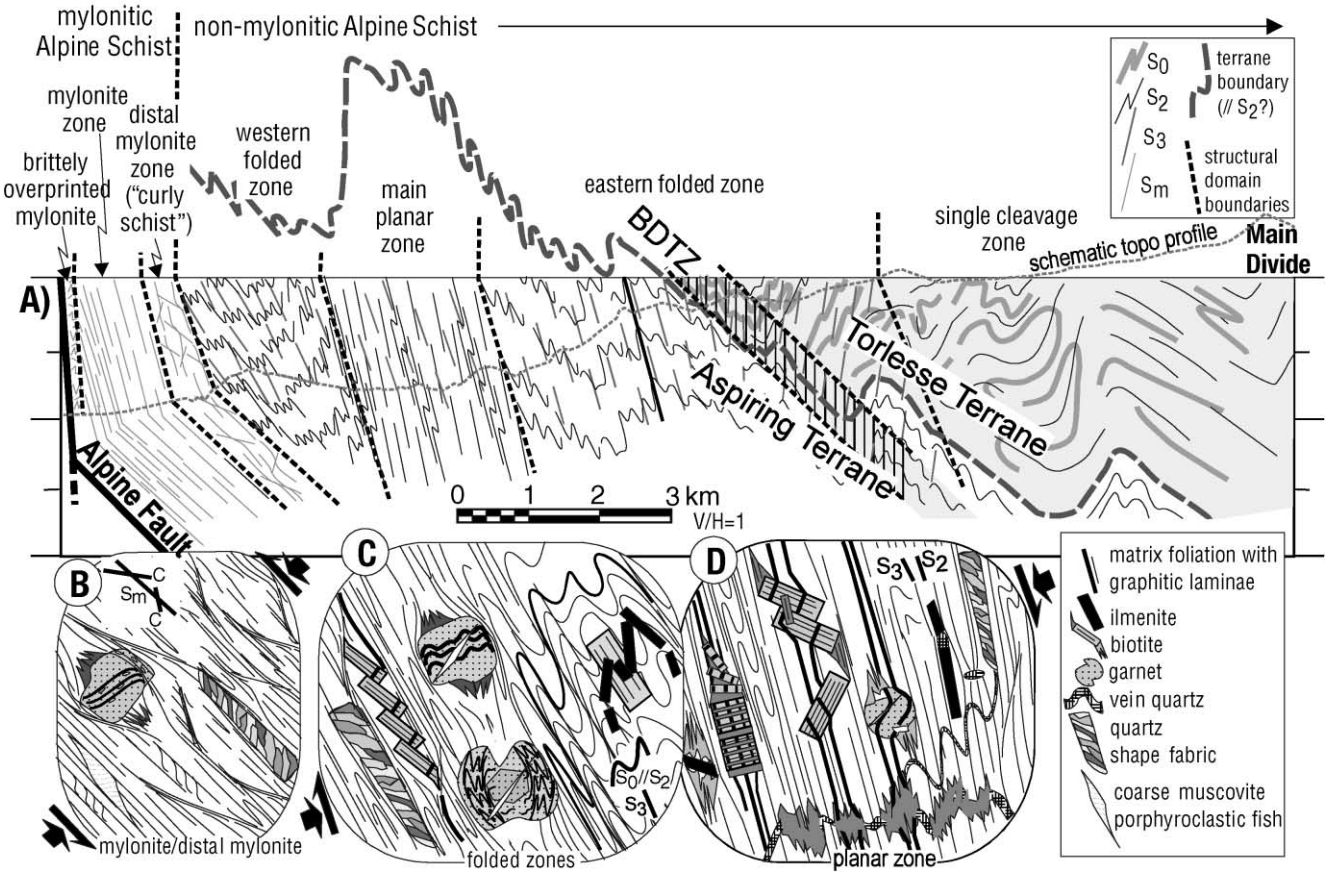

Fig. 4. (a) Schematic cross-section through the Alpine Schist in the Franz Josef Glacier–Whataroa Rivers area, New Zealand, showing major structures, fabric relationships and selected microstructures and strain gauges. Insets show typical microstrcuctures in (b) mylonitic rocks; (c) non-mylonitic folded zones; and (d) planar zones.

SE-tilted section through the middle to upper crust of the Pacific Plate (Fig. 2a). In the study area, Little et al. (2002) have divided these amphibolite to greenschist facies rocks, the Alpine Schist, into several zones based on differences in their deformational fabrics and microstructures (Figs. 3 and 4a). Dextral-reverse shear fabrics occur in mylonitic rocks that crop out <2 km from the Alpine Fault; these are cataclastically deformed within ~30–100 m of the fault (Sibson et al., 1981; Norris and Cooper, 1995). Protomylonites form a transition between mylonitic and non-mylonitic parts of the Alpine Schist (Fig. 4b, distal mylonite zone).

The non-mylonitic part of the Alpine Schist contains two foliations: an early one (S_2) that broadly dips SE, and a near-vertical crenulation foliation (S_3). The latter foliation, referred to as the Alpine foliation, strikes ~15° oblique to the Alpine Fault and initially developed during Barrovian metamorphism of the Alpine Schist at least 20 m.y. before the modern (<6.4 Ma) phase of oblique plate motion (Little et al., 2002). Microstructures, such as inclusion trails, indicate that most garnet porphyroblasts and some biotites nucleated during early phases of Alpine foliation development, but that biotite grains continued to nucleate and grow into the late Cenozoic subsequent to this. The hinges and gently dipping limbs of kilometre-scale folds of the early foliation are abundantly crenulated and mesoscopically folded (folded zones, Fig. 4a and c), whereas their near-vertical limbs contain planar fabrics (Fig. 4d). In the latter, the early foliation and its differentiated layering have been steepened into subparallelism with the Alpine foliation, leading to their layer-parallel stretching. The Alpine foliation dies out near the top of the structural pile near the Main Divide, where the early foliation (S_2) is the sole cleavage in the rocks (single cleavage zone, Fig. 4a).

In the late Cenozoic, S_3 was intensified during its passage through the Southern Alps orogen and exhumation along the Alpine Fault (Little et al., 2002). One expression of this reinforcement is spectacular bookshelf sliding and micro-boudinage of lath-like biotite porphyroblasts (Fig. 4d). Thermochronological data imply that ductile fabrics on the hanging wall of the Alpine Fault were 'frozen in' at the brittle-ductile transition zone at only ~1–3 Ma (e.g. Batt et al., 1999, 2000). At Franz Josef Glacier, a fossil brittle-ductile transition zone is exposed in biotite-zone rocks ~7 ± 1 km structurally above the Alpine Fault (Little et al., 2002). Deformed quartz veins below this zone (BDTZ, Fig. 4) preserve a late Cenozoic grain-shape fabric that is not present above it. The 1–2-km-wide BDTZ is pervaded by systematically spaced, vertical shear zones

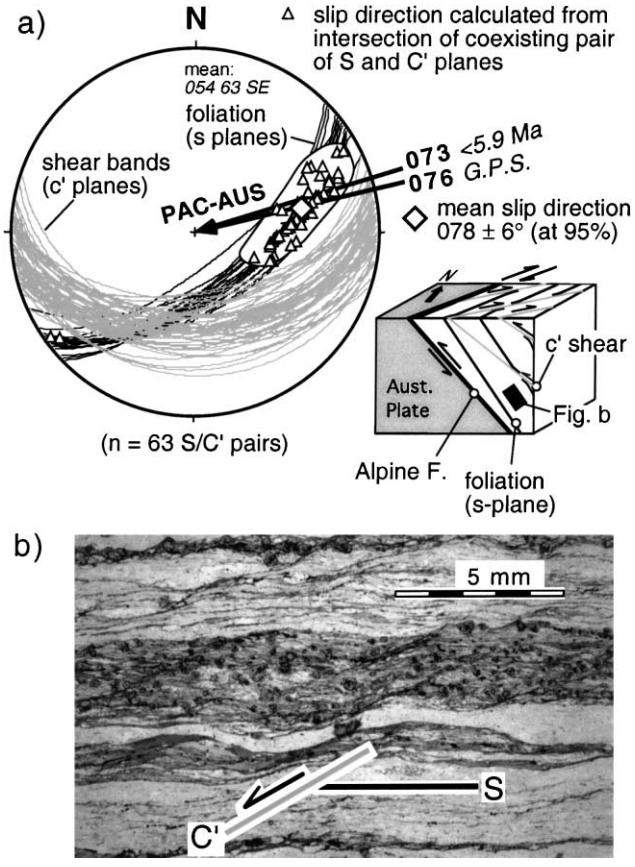

Fig. 5. (a) S/C' shear-band fabrics at Tatare Stream locality near Franz Josef Glacier (Fig. 2a). The bulk shear direction was calculated as the perpendicular to the intersection lineation of the S and C' planes that lies in mylonitic foliation plane (= subparallel to the Alpine Fault). (b) Photomicrograph (plain light) of oblique (S/C') shear bands in mylonitic micaceous quartzite or metachert from the distal Alpine mylonite zone ('curly schists') in Tatare Stream. Approximate orientation of photograph is shown by black box on block diagram in (a). Dark high relief grains are garnet.

striking subparallel to the Alpine Fault. These discrete shears have a dextral-oblique sense of slip with a down-to-the-east sense of throw, antithetic to the Alpine Fault, as do pervasively developed ductile shear indicators in non-mylonitic Alpine Schist structurally below the BDTZ (Holcombe and Little, 2001; Little et al., 2002).

4. Transport direction in distal Alpine mylonites

We measured the direction of shear in the distal mylonite zone in Tatare Stream near Franz Josef Glacier, <750 m from the Alpine Fault (Fig. 3), by analysing the orientation and kinematics of oblique shear bands (S/C' fabrics) in micaceous quartzites. The shear bands resemble the banded type of S–C' fabrics described by Blenkinsop and Treloar (1995), with the micaceous foliation surfaces (S) being more conspicuous than the oblique shear bands (C') deflecting those folia. Although conjugate shear bands occur, most shear bands (C' shears) dip less steeply SE than the mylonitic foliation (S_m), and record a dextral-reverse sense of shear that is synthetic to the Alpine Fault (Fig. 5a). The ductile shears are spaced at 1–3 mm (Fig. 5b). The attitudes of 63 pairs of S and C' planes define a mean dihedral angle, δ, of $32 \pm 7°$ (1σ). In the plane of the mean mylonitic foliation (S_m), the perpendicular to the mean S/C' intersection lineation trends $078 \pm 6°$ (±two standard errors), indicating a shear direction that is statistically indistinguishable from Pacific–Australia plate motion vectors defined by both Nuvel-1 and G.P.S. data. This result was duplicated by Wightman (2000) at other sites in the mylonite zone ~20 km to the SW near Fox Glacier (mean slip direction $072 \pm 6°$ based on a sample of 20 S/C' pairs). These data provide an important velocity boundary condition for ductile deformation in the hanging wall of the Alpine Fault.

5. Measures of finite and incremental strain in non-mylonitic Alpine Schist

5.1. Foliation-orthogonal shortening

Linear shortening perpendicular to the Alpine foliation (S_3) can be estimated from the folded shape of marker layers and from several types of microstructural strain gauges. Holm et al. (1989) used the sinuous bed method and Talbot's (1970) technique to estimate 50–75% foliation-orthogonal shortening of ptygmatically folded quartz veinlets deformed across the Alpine foliation (S_3) in the main planar zone at Franz Josef Glacier (Fig. 4a). They inferred that these veins were emplaced in the late Cenozoic (<10 Ma). We have estimated foliation-orthogonal shortening by measuring the buckled shape of ilmenite platelets transverse to S_3 (Figs. 4c and 6a, inset). Microstructural observations indicate that most of the 0.2–3-mm-long ilmenites grew after formation of the early foliation (S_2), which is preserved in them as quartz inclusion trails (e.g. Fig. 8d), and prior to D_3 crenulation folding. Grains confined to a single microlithon domain were not measured. This application of the sinuous bed method yields a minimum estimate of bulk shortening since ilmenite growth. Bulk shortening is underestimated because of marked strain partitioning around the stiff ilmenite porphyroblasts, as evidenced by wrapping of foliation around the grains and by increased appression of microfolds external to the ilmenites. Although the mean ilmenite shortening value that we measured was ~60% (Fig. 7), due to the problem of underestimation, we believe that our higher strain estimates ($e = -70$–80%) are nearest to the actual value of bulk strain since ilmenite growth. Note that these minimum strain values are indistinguishable from those reported by Holm et al. (1989) for shortening of their 'late stage' quartz veins. They are also comparable with three estimates of fold-related shortening of laterally continuous quartz segregations parallel to the early foliation, which ranged from 65 to 73% (Fig. 4a).

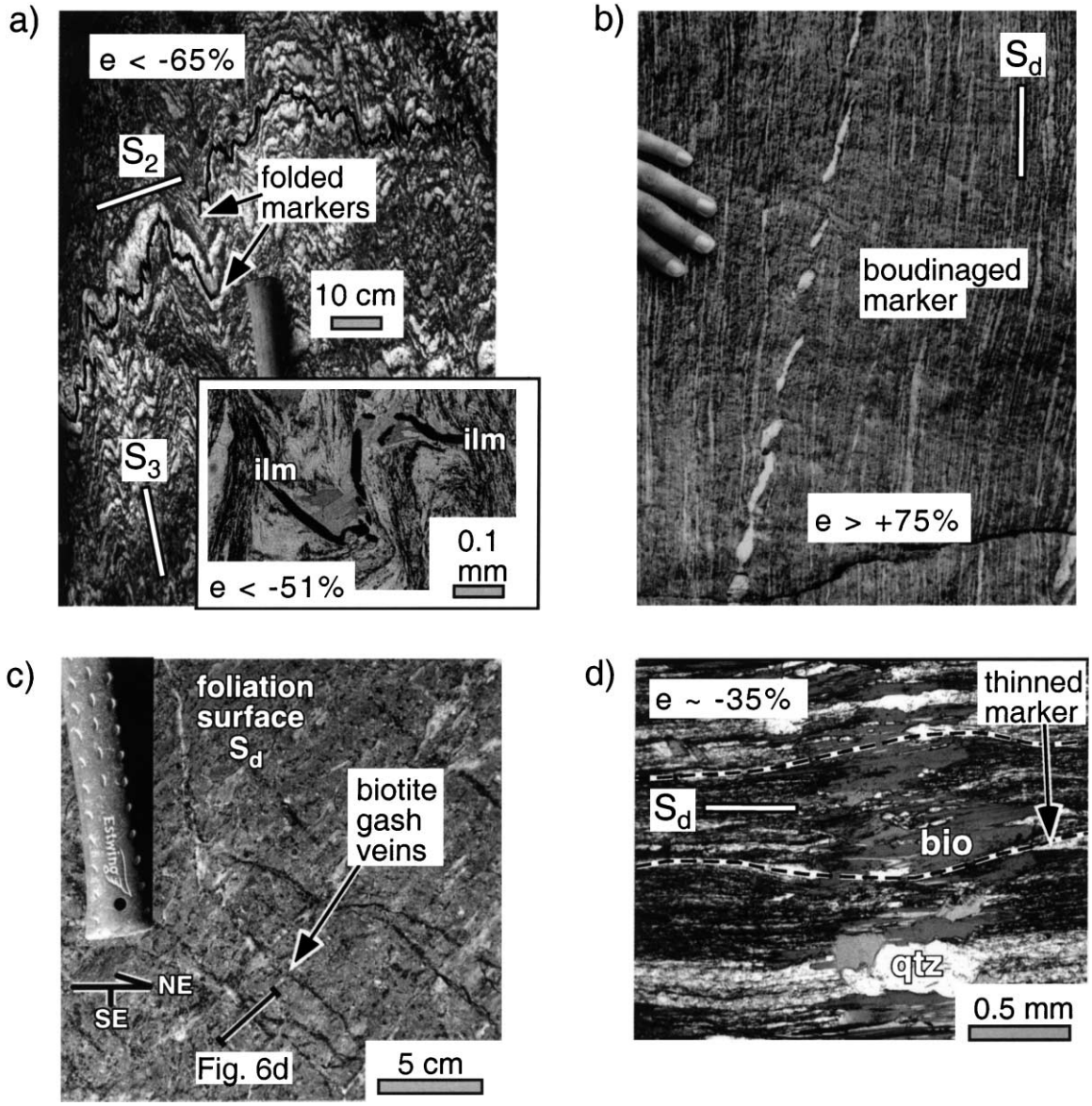

Fig. 6. Photographs of selected strain markers. Where specified, longitudinal strain values are quoted in percent (+ve extension, −ve contraction). (a) Down-plunge view of folded zone showing sinuous trace of deformed early foliation (S_2). Dark lines denote the traces of three quartz segregations that together have been shortened by over 65%. Inset shows photomicrograph of crenulated rock with buckled ilmenite plates. (b) Oblique boudinage of deformed quartz vein (main planar zone, Franz Josef Glacier). Note that this vein's apparent extension of 75% is an underestimate of the maximum finite extension in 3D because of the 2D nature of the outcrop and the obliquity of the vein to the foliation trace; also, boudinage records only part of the layer-parallel extension. (c) Photograph of foliation surface showing trace of biotite gash-veins (main planar zone, Franz Josef Glacier). (d) Photomicrograph, perpendicular to foliation, showing profile of biotite-gash vein with graphite-rich inclusion trails (plain light). Note sinuous trace of vein and evidence for post-vein shortening of matrix laminae relative to corresponding inclusion trails in the biotite.

A more precise measure of foliation-orthogonal shortening in the Alpine Schist is provided by changes in the width of graphitic and quartz-rich laminae that can be traced continuously from the matrix into the cores of porphyroblasts, where they are preserved as inclusion trails (Figs. 8a and 9a). Linear regression for the best-fit ratio of the internal to external widths of these markers suggests a mean of ~50% shortening since growth of garnet (Fig. 9d). Differential thinning across individual garnets records a post-growth shortening that is locally as much as 68% or as low as ~20% (Fig. 9e). Biotites (Fig. 9c) typically record less shortening (mean is ~30%), but they also display a larger range of shortening values, from as high as 59% to as low as ~10% (Fig. 9f). These relationships are not surprising given that biotite growth outlasted that of garnet, and that several generations of biotites are recognised microstructurally, with the youngest growing in the late Cenozoic mylonitic fabric (Little et al., 2002). Because ilmenite commonly occurs as inclusions in garnet, it is not unexpected that our estimates of bulk shortening since

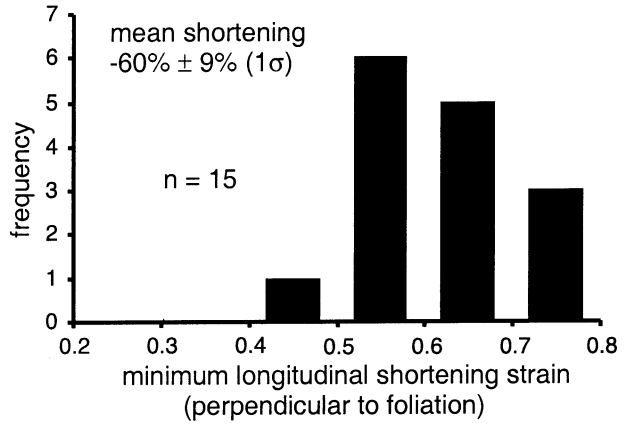

Fig. 7. Histogram of 15 foliation-perpendicular shortening strains measured using the deformed shape of microbuckled ilmenite platelets in non-mylonitic Alpine schist (garnet and biotite zones). These are minimum estimates of bulk shortening perpendicular to the foliation, and we infer that the highest strains measured ($e = -0.7$ to -0.8) come closest to the true value.

ilmenite growth (>70%) are greater than that those since garnet (~50%).

Another estimate of foliation-orthogonal shortening is based on bookshelf sliding of internally deformed biotite porphyroblasts (Figs. 4c and d and 8b). Internal inclusion trails of the S_2 foliation within the biotites provide a record of the initial angle of biotite grains to the foliation. Together with measurements of the final angles of the bookshelf packets to the foliation, these data can be used to estimate the amount of foliation-orthogonal shortening accommodated by splitting and rotation of the cleavage packets (Fig. 9b). The likelihood of out-of-plane rotations in a given thin-section mean that the measured apparent rotations in 2D are probably an underestimate of the actual rotation and shortening strain. We derived a mean shortening value of 42% using a wide range of thin-section orientations perpendicular to the foliation (Fig. 9g). The shortening does not vary in any obvious way with pitch of the thin-section in the foliation plane. In detail, the data may be bimodal. One mode, possibly corresponding to earlier biotite grains, records shortenings of ~50%, similar to values based on differential thinning of laminae across garnets and some biotites. The other apparent mode corresponds to ~30–40% shortening. Some estimates are as low as ~10–20%.

The variation in post-biotite shortening increments may reflect strain differences between biotites of differing age. In addition to the variation in bookshelf-related shortening strain, a range of post-biotite shortening strains are recorded by the lamination width data for biotite (Fig. 9f). Although some of the biotite width data indicates up to 55% shortening, in broad agreement with garnet width data and some estimates based on bookshelf-rotated biotite grains, the majority indicate less than 50% of post-biotite shortening, and values as low as 20% are common. Interestingly, both the bookshelf-rotation and lamination width data sets for biotite suggest that there are groups of biotite grains experiencing ~50, ~30–40, and ~20–25% shortening since their growth (Fig. 9f and g). If real, these modes may reflect discrete phases of nucleation of biotite grains.

5.2. Foliation-parallel extension

Linear estimates of extension in the Alpine Schist since porphyroblast growth are provided by strain shadows and microboudins. Strain shadows adjacent to garnet and ilmenite porphyroblasts are filled antitaxially by nonfibrous intergrowths of plagioclase, muscovite, biotite, quartz and chlorite, with the latter two being most common proximal to the garnet (Little et al., 2002). The tapered shape of the shadows indicates they were deformable. We measured garnet strain shadows in 112 thin-sections of Alpine Schist (Fig. 10). In each, we measured the relative elongation of 4–12 garnet strain shadows to derive a mean for that thin-section. The 'cut effect' associated with 2D sampling of these 3D objects, and the likelihood that some extension was not recorded in increments of strain shadow growth, means that these are minimum estimates of foliation-parallel stretch since growth of garnet. Results indicate that the several garnet-bearing non-mylonitic zones in the Alpine Schist each experienced a similar mean foliation-parallel stretch of ~2.0 (= 100% extension). Boudinaged quartz veins in the schist record minimum extensions that also locally approach this value (Fig. 6b). Importantly, extensions do not vary obviously as a function of thin-section pitch in the foliation (solid squares, Fig. 10), an indication that the shadows have a pancake-like shape in 3D (Fig. 11b). If deformation was isovolumetric, a perfectly oblate finite stretch of 2.0 implies a foliation-normal post-garnet contractional stretch of 0.25 (i.e. shortening strain of ~75%). Chlorite-infilled strain shadows near ilmenite grains typically record an ~2:1 foliation-parallel stretch similar in magnitude and apparent oblateness to those adjacent to garnets (Fig. 8d).

Microboudinaged biotite grains provide a measure of foliation-parallel stretch since growth of those porphyroblasts. Typically, microboudinage affects elongate biotites that have their (001) cleavages at a high angle to that fabric (Fig. 4d). Microboudins of biotite are ubiquitous throughout garnet zone and higher grade rocks, and are seen in all orientations of thin-section cut perpendicular to the foliation plane, a relationship indicative of an oblate finite strain. Microboudinaged fragments of the original grain can be recognised by their graphitic inclusion trails, whereas new biotite grains syntaxially filling the dilation zones between separated cleavage fragments are inclusion-free (Fig. 8c). Measurement of the cumulative widths of these two optically distinct phases allows a minimum foliation-parallel stretch of the microboudinaged grain to be calculated (Fig. 10, open circles). The mean extensional stretch calculated from analysis of 22 foliation-perpendicular thin-sections containing such microboudinaged grains is ~1.4. For an

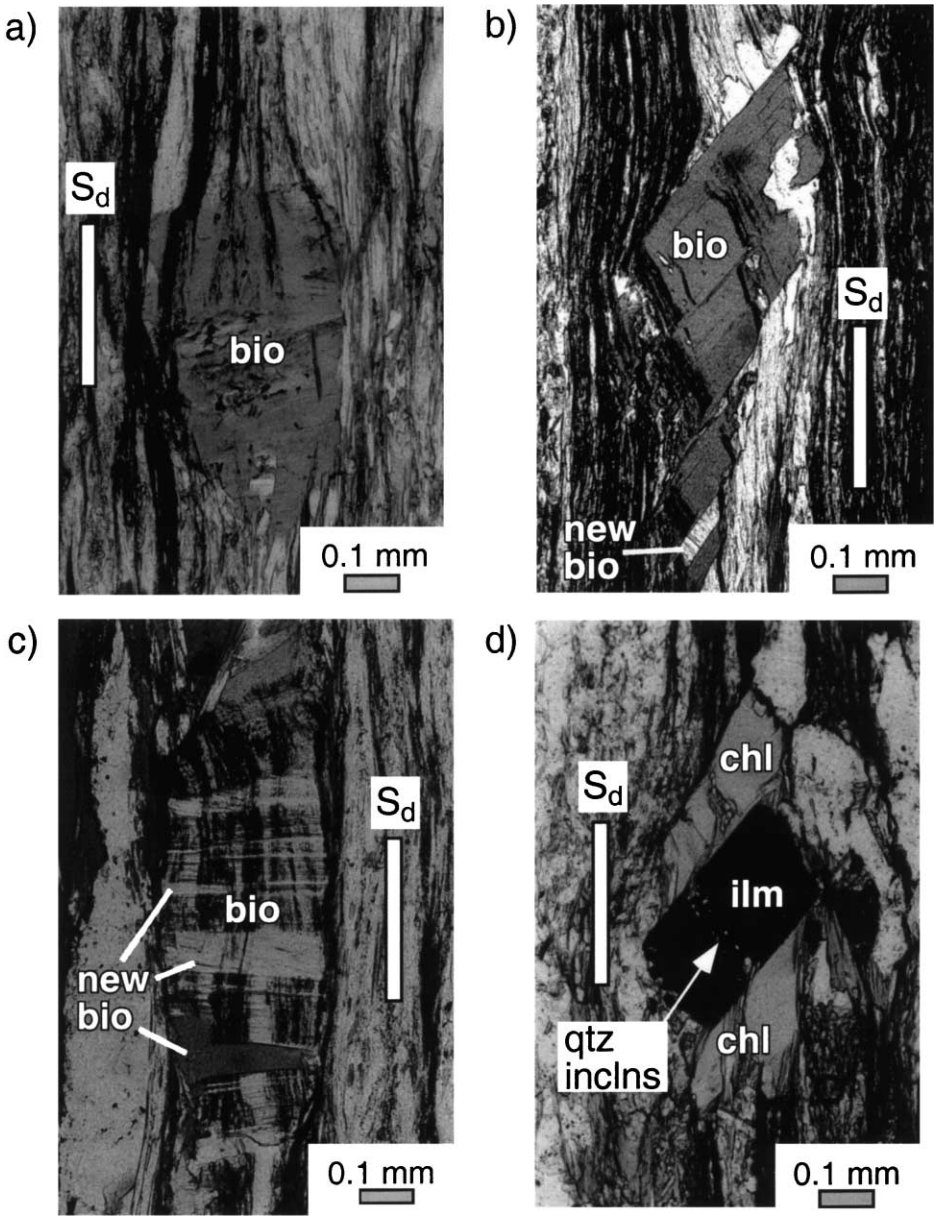

Fig. 8. Photomicrographs (all in plain light) of grain-scale strain gauges used in this paper. Abbreviations: 'bio' refers to biotite; 'ilm' to ilmenite; and 'chl' to chlorite. 'S_d' is dominant foliation in the sample (= Alpine foliation, S_3, except in S_2 planar zones). (a) Differential thickness of graphitic marker laminae inside vs. outside of porphyroblasts; (b) bookshelf tiling and rotation of biotite porphyroblasts that preserve inclusion trails of the external foliation; (c) microboudinage of inclusion-rich biotite laths. Dilational infillings between boudin fragments are clear; and (d) strain shadows.

isovolumetric, perfectly oblate strain, this stretch would correspond to a foliation-orthogonal shortening of ~51%.

5.3. Oblate shape of finite strain

Ductile fabrics in the Alpine Schist contain abundant evidence for an oblate shape of both finite and late-incremental strain. Holm et al. (1989) used the subequal abundance of subhorizontal and subvertical extension fractures in garnet-zone rocks near Franz Josef Glacier to argue that the minimum and intermediate principal stresses were subequal in magnitude during brittle hydrofracturing. They also reported an oblate shape of finite strain by application of Talbot's (1970) method to ductilely folded vs. boudinaged quartz veins in the main planar zone. As mentioned above, the circular shape of garnet strain shadows, and biotite microboudins observed in diverse orientations of thin-sections also reflect oblate strain.

Extension fractures, typically lined with chlorite, split garnet grains both in the mylonite zone (Prior, 1993) and in the non-mylonitic section. In thin-section, fractures have straight traces that are typically disposed at a high angle to the foliation, and commonly they are statistically orthogonal

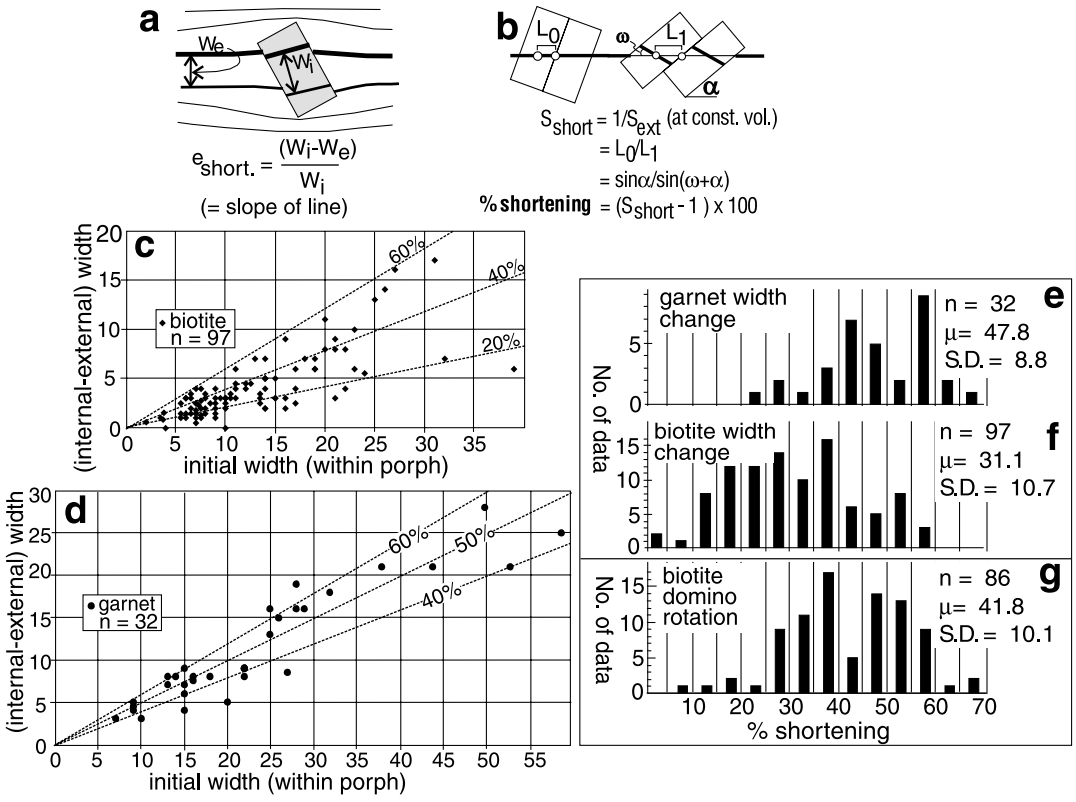

Fig. 9. Estimates of foliation-orthogonal shortening based on (a) differential thickness of graphitic laminae inside (*Wi*) vs. outside (*We*) of porphyroblasts, and (b) bookshelf rotation of biotites. Assuming area conservation, measurements of the angle of internal inclusion trails to foliation (ω) and final angle (α) of rigid bookshelf sliding packets can be used to estimate foliation-orthogonal shortening strain. Scatter plot for garnet porphyroblasts (c) graphs the internal thicknesses of graphitic marker laminations (*Wi*) in biotite against their external thickness (*We*). Reference slopes for 40, 50, and 60% shortening strains are shown as dashed lines. Scatter plot (d) presents similar data for garnet porphyroblasts. Histogram (e) plots frequency against individual strain estimates based on changing lamination widths across garnet grains. Histogram (f) plots similar data for biotite grains. Histogram (g) plots frequency against individual shortening estimates based on bookshelf rotation of biotites.

to it. Most fractures are transgranular without penetrating the adjoining matrix (Fig. 11b). Serial thin-sectioning reveals that fractures are distributed zonally around the foliation pole (Palmer, 2000). Dilatation across these 1–300 mμ wide, extension cracks expands garnet grains radially in the foliation plane. While planar fabric anisotropy probably contributed to development of these foliation-orthogonal fractures (e.g. Ji et al., 1997), their zonal disposition records an oblate incremental strain.

Further evidence for an oblate (radial) pattern of extension in the steeply dipping Alpine foliation is provided by boudinage structures that are abundant on both horizontal and vertical outcrop surfaces (Fig. 11a). Especially common in planar zones, foliation boudinage is accommodated by slip on conjugate shear bands and by dilational necking associated with quartz–biotite or quartz–chlorite–calcite veins. Glaciated exposures reveal a chocolate-tablet arrangement of boudins in that steep foliation (see Holm et al., 1989).

Another index of strain shape is provided by shape fabrics of recrystallised quartz grains in deformed veins at deep levels of the Alpine Schist beneath the fossil late Cenozoic BDTZ (Fig. 4a). Foliation-parallel thin-sections have equant quartz grain-shape fabrics, whereas sections perpendicular to the foliation have elongate fabrics parallel to the foliation (Fig. 11c and d). Finally, oblate strain in the Alpine Schist is expressed, we believe, by the indistinctness of stretching lineations in both the mylonitic and non-mylonitic parts of the Alpine Schist. As recognised by Sibson et al. (1981), elongation lineations are typically indistinct in Alpine Schist mylonites except in bands of quartz-rich schist or metachert, in which a mylonitic lineation pitches NE. Variable lineation development may reflect decimetre-scale partitioning of simple shear into the quartz-rich layers, which become *LS*-tectonites, with the surrounding micaceous rocks undergoing transpressive flow to become *S*-tectonites. This inference is supported by quartz *c*-axis lattice preferred orientation data (Ilg and Little, 1999). In the micaceous mylonites, sub-simple shear flow is also implied by the locally conjugate nature of shear band development in both the mylonite and distal mylonite zones (Fig. 4b). These fabrics suggest extension parallel to the Alpine Fault.

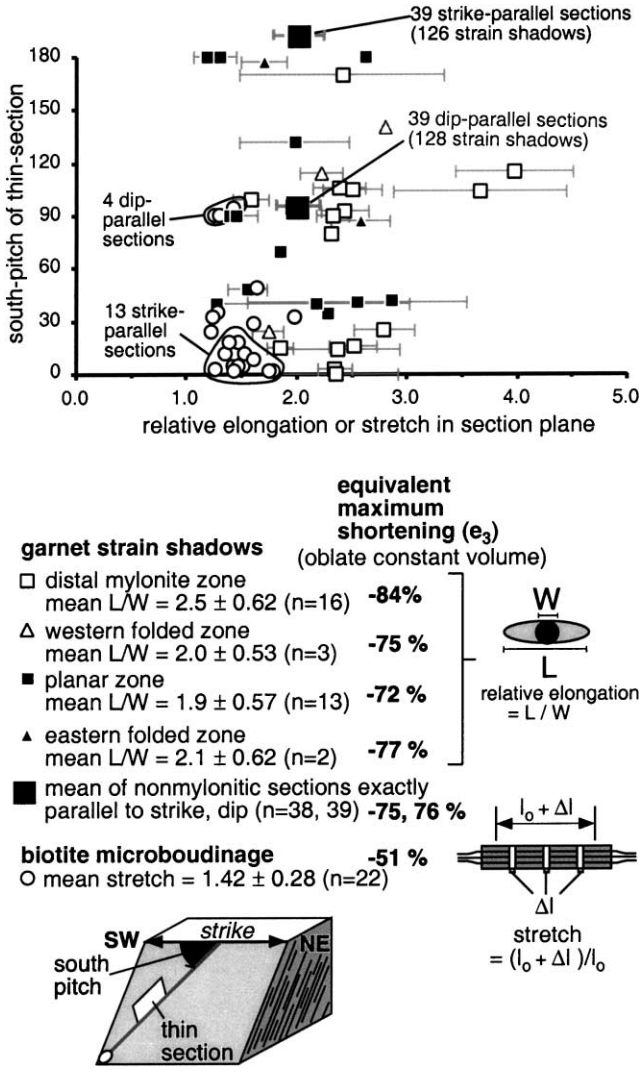

Fig. 10. Estimates of foliation-parallel stretch in non-mylonitic rocks of the Alpine Schist plotted as a function of pitch of the observed thin-section in the Alpine foliation plane. The relative elongation of strain shadows or microboudins provides a minimum estimate of foliation-parallel stretch. Distinct symbols are used to plot results from different structural zones. Sample number, n, is the number of thin-sections examined in each zone (each ~1–5 km wide). In each section, a mean elongation was derived by averaging the 4–12 most distinct strain shadows or microboudins. The quoted standard deviations (1σ) refer to the variation in means for all the samples in that zone. Equivalent maximum shortening strains for each zone are based on assumption of constant volume deformation and perfectly oblate strain. Data for strike and dip-parallel strain shadows (solid boxes) are from Palmer (2000).

5.4. SW-pitching stretching direction in non-mylonitic Alpine Schist

A stretching direction is not conspicuous in the mesoscopic rock fabric of the Alpine Schist. In folded zones, the dominant lineation is an intersection, $L_{2\times3}$, between the early foliation and the steeply dipping Alpine foliation (Little et al., 2002). By definition, these SW-pitching crenulation hinges are not stretching lineations. In the main planar zone at Franz Josef Glacier, a quartz rodding lineation on S_2 is statistically parallel to $L_{2\times3}$. These rods are at least in part inherited from D_2.

Despite an overall oblateness of strain in the Alpine Schist, some non-mylonitic rocks preserve evidence for a maximum direction of finite or incremental stretch. These include mineral lineations, fibrous gash veins, and elongated strain shadows or quartz grain-shape fabrics. In the field, the long dimension of hornblende and biotite grains are sprayed, but define a weak to distinct lineation in the foliation plane. By scanning foliation plates and digitising mineral grains, we measured the orientation distribution of elongate hornblende and biotite crystals on the foliation surface in garnet zone rocks. Analyses after Masuda et al. (1999) confirm that a statistically significant lineation is generally present. Mineral lineations typically pitch moderately SW to down-dip (open circles Fig. 12). We interpret these to approximate the direction of maximum finite stretch in the non-mylonitic Alpine Schist.

Biotite-infilled gash veins intersect the steeply dipping foliation plane in abundant, ribbon-like traces <1 cm wide (Fig. 6c). In profile, the nonfibrous veins are approximately perpendicular to the foliation, sinuous, and track folded quartz veinlets (Figs. 4d and 6d). Coarse biotite infilling these dilational veins grew poikiloblastically beyond vein walls to include graphitic laminations from the wall rocks. Post-vein shortening (~30%) is recorded by wrapping of the foliation around isolated vein segments and by lamination width differences between the internal and external parts of the veins. Vein poles record incremental stretches pitching moderately SW (solid dots, Fig. 12a). Because the fibres are approximately parallel to $L_{2\times3}$, we cannot rule out the possibility that elastic anisotropy controlled the orientation of maximum tensile stress in the rocks. If elastic stiffness and fibre stress were at a maximum parallel to the lineation, fracturing may have occurred perpendicular to the lineation despite an overall oblate ductile strain.

The locally inequant shape of strain shadows and quartz grain-shape fabrics provide further evidence for a SW-pitching direction of maximum incremental stretch in some samples. We compared the apparent elongation of strain shadows and quartz grain-shape fabric as a function of thin-section orientation by inspection of pairs of orthogonal sections cut perpendicular to the foliation. The mean aspect ratio of garnet or ilmenite strain shadows or quartz grain-shape was statistically more elongate (at two standard errors) in one plane than in the other plane in 50 of the 150 orthogonal pairs examined. Most of these apparent stretching directions lie in the SW-pitching quadrant of the Alpine foliation (Fig. 12b). A more precise way of identifying directions of maximum incremental stretch is by digitising and statistically analysing quartz-grain shape fabrics on three mutually orthogonal planes, including one parallel to the foliation. We quantified the orientation distribution of the long directions of recrystallised quartz grains in monomineralic, deformed quartz veins below the fossil BDTZ.

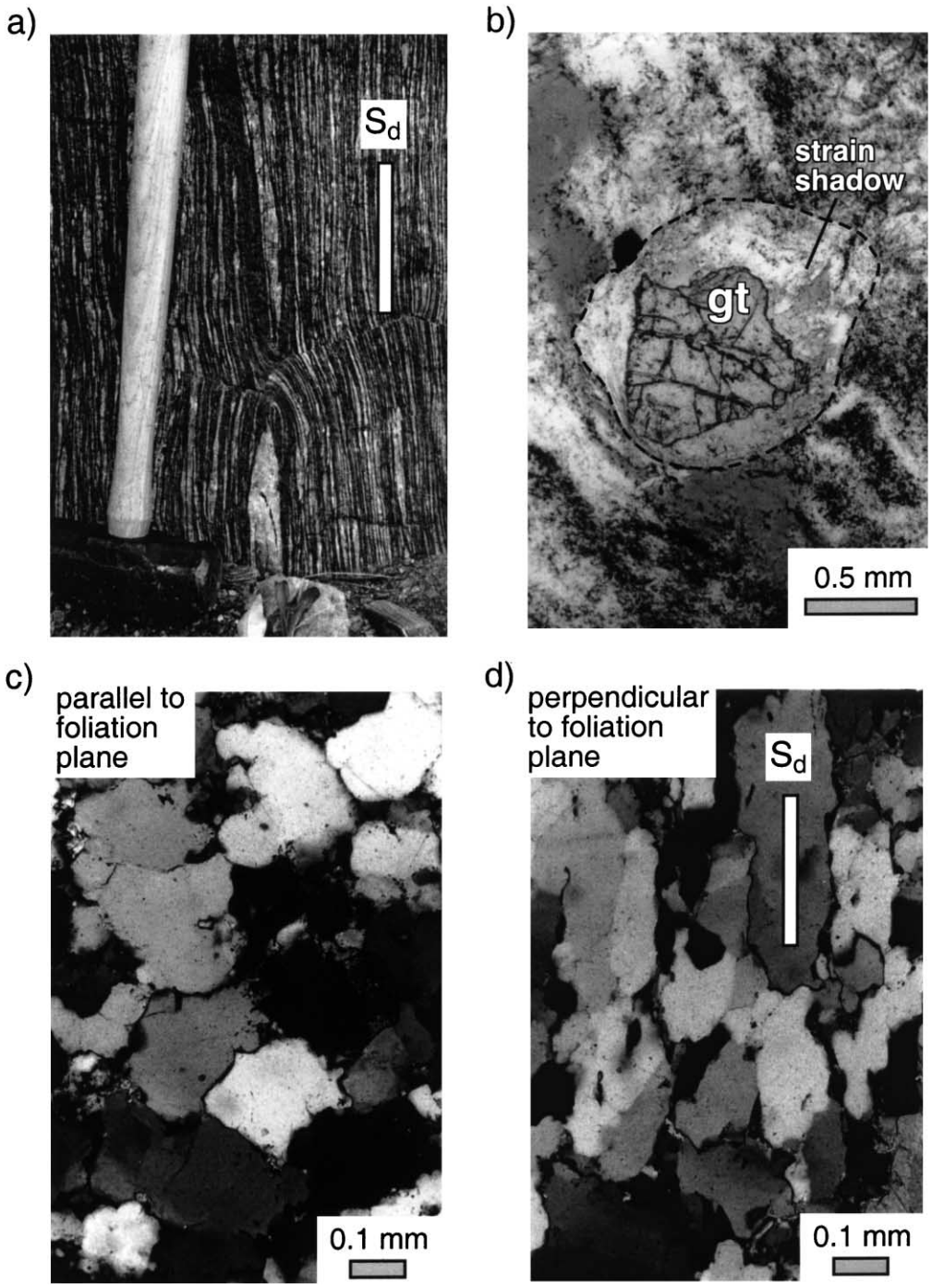

Fig. 11. Evidence for oblate finite strain in the Alpine Schist. (a) Photograph of foliation boundinage on vertical outcrop face in the main planar zone at Franz Josef Glacier (garnet zone). These structures are also common on horizontal outcrop surfaces, suggesting a chocolate tablet style of boudinage. (b) Strain shadow surrounding internally fractured garnet in section cut parallel to foliation showing radial pattern of extension. Plain light. (c) Equant quartz grain-shape fabric in deformed quartz vein in thin-section cut parallel to foliation from main planar zone, Whataroa River. Crossed polars. (d) Elongate grain-shape fabric in thin-section cut perpendicular to foliation in the same sample. Comparison of (c) and (d) strongly suggests an oblate finite strain since recrystallisation of the quartz vein.

Despite the oblateness of the post-recrystallisation incremental strain (Fig. 11c), preliminary grain-shape fabric analysis of 15 samples reveals an elongation direction that plunges moderately to steeply SW.

5.5. Inferences about strain path

The Alpine foliation accumulated during at least two phases of deformation. Little et al. (2002) argued that an

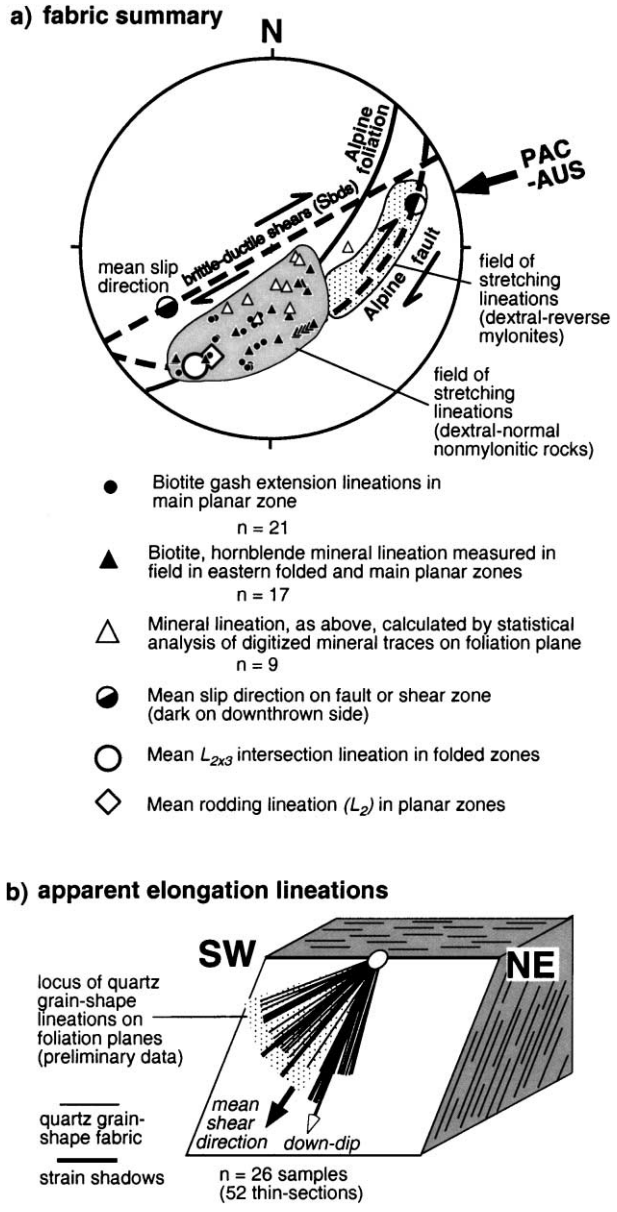

Fig. 12. (a) Lower hemisphere, equal-area stereogram, showing elongation lineations from Alpine (D_3) fabrics in garnet zone Alpine Schist. Also shown are the mean attitude of the Alpine Fault and its mylonitic shear direction (Fig. 5), the azimuth of Pacific–Australia plate motion in the central Southern Alps (Walcott, 1998), the mean attitude of the Alpine foliation, and the mean attitude of brittle-ductile shear bands near Franz Josef Glacier (from Little et al., 2001). Statistically determined mineral lineations (open triangles) are from Palmer (2000); (b) Block diagram plotting directions of apparent elongation in the Alpine foliation plane as inferred from comparative quartz grain shape fabrics and garnet strain-shadow elongations in orthogonal pairs of thin-sections perpendicular to the foliation. Apparent extension directions were observed in 28 of 50 pairs of thin-sections of non-mylonitic Alpine Schist. Stippled field of quartz grain-shape lineations was determined by image analysis of quartz grain-shape fabrics in deformed veins in 15 foliation-parallel thin-sections of non-mylonitic Alpine Schist (Little, unpub data). All other samples yielded mean shape fabrics that are statistically oblate. The large black arrow is a projection of late-stage (oblique normal) ductile shear direction on the Alpine foliation plane (from Little et al., 2001).

initial phase of Cretaceous or early Cenozoic age (their D_3) originally formed that steep fabric (see also Grindley, 1963; Findlay, 1987; Craw et al., 1994), whereas a younger phase (D_4) constructively reinforced it during late Cenozoic oblique convergence in the Southern Alps (see also Holm et al., 1989). Uplift and exhumation of Alpine Schist rocks through the brittle-ductile transition zone has only taken place during the past ~1–3 m.y. (e.g. Batt et al., 1999, 2000).

The differences between our various estimates of strain support the inference of Little et al. (2002) that ductile strain began after D_3 nucleation of ilmenite and garnet porphyroblasts, and that it continued to accumulate during growth of later generations of biotite grains into the late Cenozoic (D_4). Because strain in the Alpine Schist is strongly oblate, a 2D Mohr Circle construction (e.g. Ramsay, 1967) is a convenient way to plot strain increments (Fig. 13). For simplicity, these are assumed to have been isovolumetric. At deep levels of the Alpine Schist D_3 and D_4 apparently superposed one another to accomplish a combined foliation-orthogonal shortening of ~75% and a foliation-parallel finite extension of ~100%. Most strain measures in the garnet-zone Alpine Schist, such as the buckled quartz veins measured by Holm et al. (1989) and the thinning of garnet laminae may include only a partial or late increment of D_3. Many of strain measures recording ~50% foliation-orthogonal shortening (and a similar magnitude of foliation-parallel extension) are thus probably hybrids that over-estimate the late Cenozoic contribution to ductile strain (Fig. 13, stippled Mohr circle). Although many of our strain measurements provide only minimum estimates, and we have been unable to date the growth of individual biotites, we infer that the abundance of post-biotite measures of foliation-orthogonal shortening in the range of ~30–40% (Fig. 9) may reflect the late Cenozoic contribution to fabric development (D_4). That oblate grain-shape fabrics developed in (originally) polygonal quartz veins below the late Cenozoic BDTZ typically have an X/Z fabric ratio of ~1.7–2.0 (T. Little, unpub. data) supports this inference. According to this interpretation, the inherited (D_3) strain component would have involved a shortening of 62% and an extension of ~60%.

6. Spatial changes in lineation orientation

Lineations in the Alpine Schist undergo dramatic changes in pitch as a function of structural distance from the Alpine Fault, but also undergo marked local changes in orientation along-strike (Fig. 14). The dominant foliation in the Alpine Schist strikes NNE with a steep to moderate SE dip, and undergoes a progressive shallowing within ~4 km of the Alpine Fault, a relationship that Little et al. (2002) ascribed to distributed shear above that structure (Fig. 15a). At >2 km from the fault, the dominant lineation in folded zones is the intersection lineation, $L_{2\times3}$, a fabric element

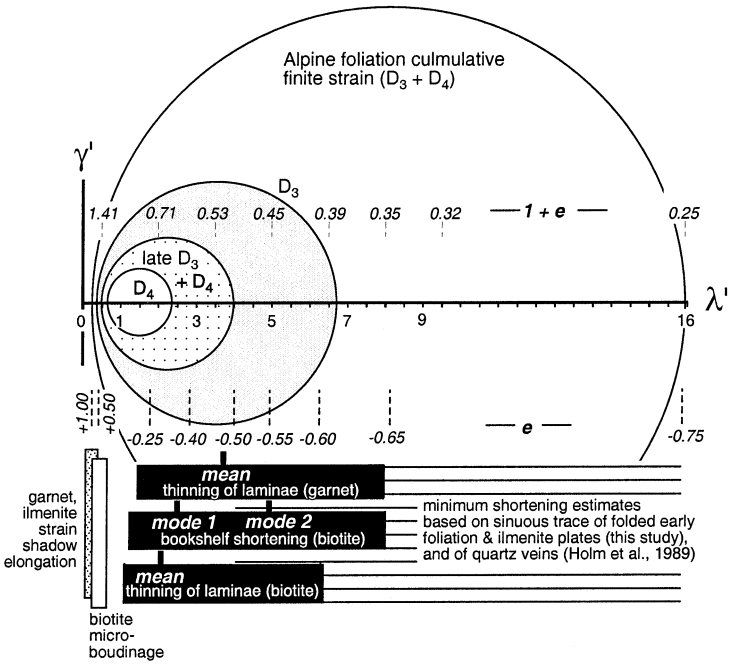

Fig. 13. Mohr circle for strain (after Ramsay, 1967) summarising available estimates of post-Alpine foliation strain accumulation in the Alpine Schist, and presenting one interpretation for the relative magnitudes of the D_3 and D_4 (late Cenozoic) increments of strain and foliation reinforcement. Note that horizontal scale of diagram is nonlinear. See text for further discussion.

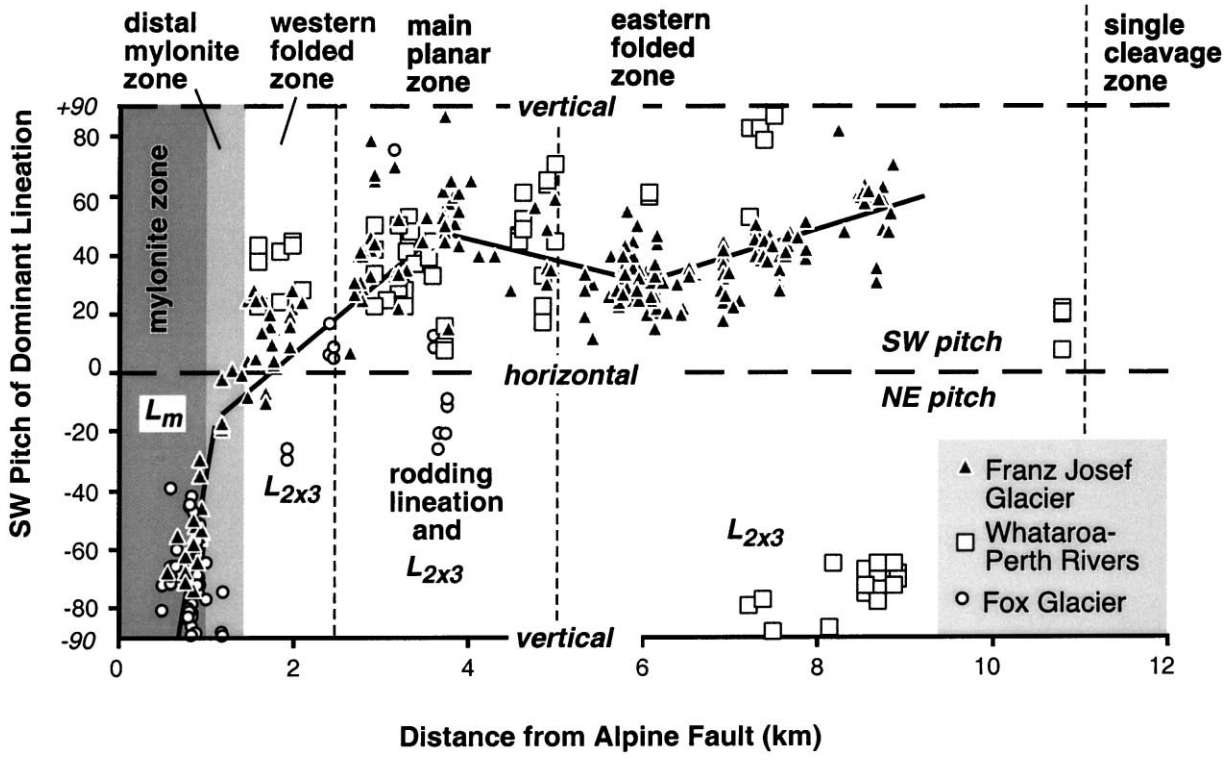

Fig. 14. Scatter plot showing SW pitch of lineations in the Alpine Schist as a function of structural distance orthogonal to the Alpine Fault plane. The figure also shows how type of dominant lineation changes across this transect. In the folded zones and eastern part of the distal mylonite zone it is the intersection lineation, $L_{2\times3}$; in the main planar zone, a D_2 rodding lineation; and in the Alpine mylonite zone, a mylonitic stretching lineation (L_m). The distance of structural data points from the Alpine Fault plane were calculated in 3D by vector algebra from map coordinates and elevations stored in a G.I.S. database. The calculation assumes that the mean trace of the Alpine Fault is as shown in Fig. 3, and that the fault dips 50° SE. Changes to these arbitrary input values would not significantly change the spatial trends displayed by the plot. Data from Fox Glacier area is from Wightman (2000).

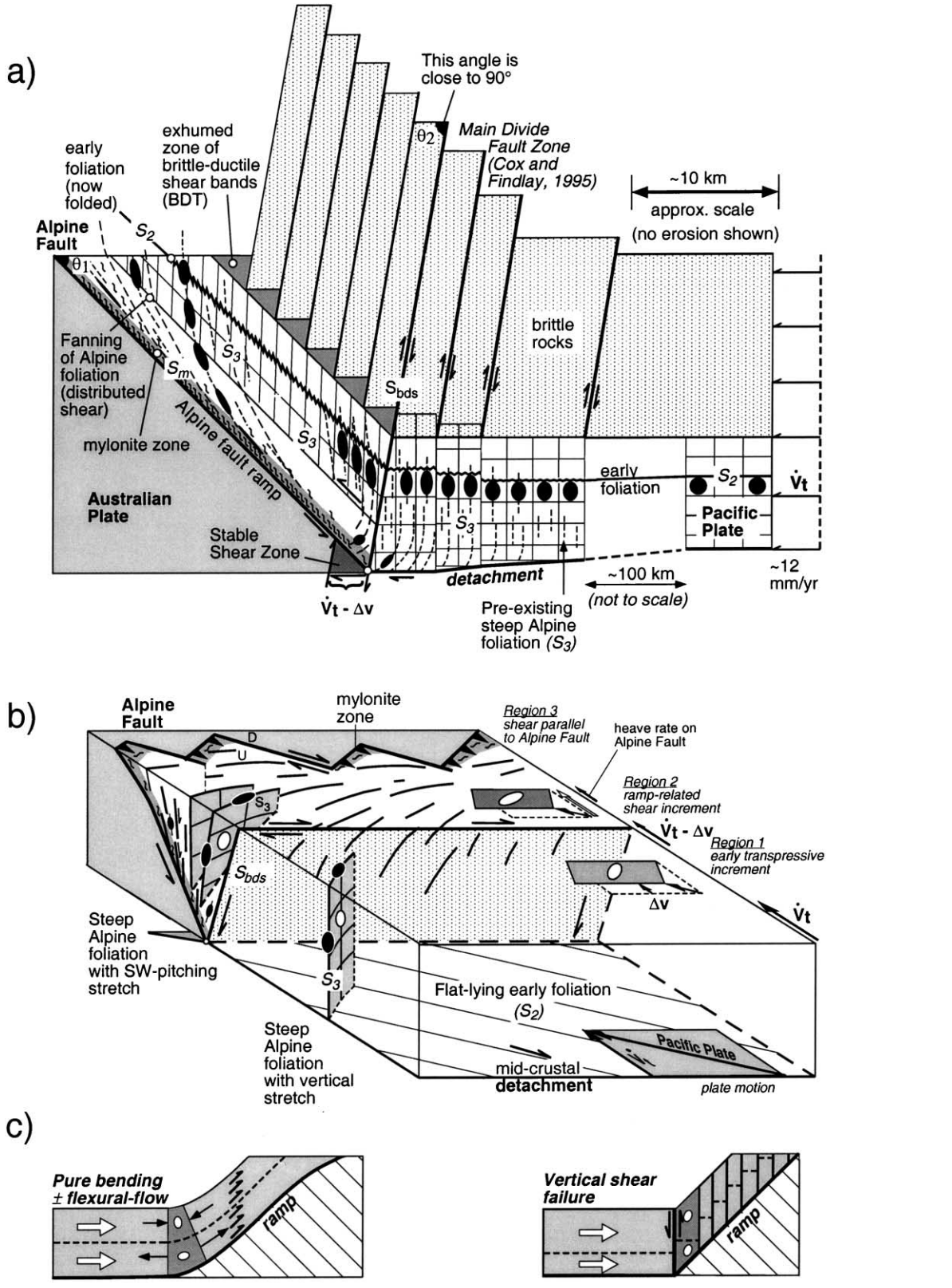

Fig. 15. Inferred kinematics of late Cenozoic deformation in the Alpine Schist, central South Island, New Zealand. (a) Cartoon showing inferred cross-sectional relationship of Alpine Schist fabrics to late Cenozoic oblique convergence between the Pacific and Australian Plates, central Southern Alps. V_t is the convergent component of plate motion. Δv is amount of convergence accommodated across outboard part of orogen. (b) Schematic block diagram showing nature and location of three deformation regions affecting middle crustal Pacific Plate rocks during oblique convergence, and their relationship to plate motions and deformational fabrics. 'S_{bds}' refers to steeply dipping shears accommodating differential uplift at oblique ramp of Alpine Fault.

inherited from D_3, whereas in planar zones the dominant lineation is a rodding lineation that may be even older. At Franz Josef Glacier, $L_{2\times3}$ pitches ~60° SW at >8 km from the fault and progressively shallows to a ~30° pitch at ~6 km from that structure. By contrast, the same lineation in the Whataroa–Perth River Valleys pitches only 5–20° SW pitch at ~11 km from the fault, steepening sharply to a down-dip or steep NE pitch at 7–9 km. A similarly near-vertical intersection lineation typifies the Alpine foliation fabric in the Kokotahi River region near Hokitika (Fig. 2a), but at ~4–5 km from the Alpine Fault (Thurlow, 1999). $L_{2\times3}$ lineations ~4 km from the fault at Franz Josef Glacier pitch ~40° SW, whereas at Fox Glacier they are subhorizontal (Fig. 14) (Wightman, 2000).

In the Franz Josef Glacier, Whataroa River, and Fox Glacier areas, the $L_{2\times3}$ intersection lineation pitches 50–20° SW at <5 km from the fault, decreasing to approximately zero (horizontal) in the eastern part of the distal mylonite zone at <2 km. Farther west in the distal mylonite zone, subhorizontal remnants of the $L_{2\times3}$ intersection lineation locally coexist with a younger NE-pitching mylonitic stretching lineation. Sibson et al. (1981) attributed the shallowing of the Alpine Schist's intersection lineation in proximity to the eastern margin of the mylonite zone as the product of a strain-related rotation of lineations towards the (NE-pitching) mylonitic stretching direction during the late Cenozoic. To accommodate the observed ~30° shallowing in pitch of $L_{2\times3}$ by means of a passive, strain-related rotation, however, would require a sectional strain ratio (X/Y) of ~4.0 near Franz Josef Glacier. This is quite unlikely, as most of the lineation pitch change takes place in non-mylonitic rocks that have a foliation-parallel strain ratio that is close to unity (oblate). Variation in the local sheet dip of the early foliation, both along and across strike of the Alpine Fault, is the most likely reason for strong local variations in the pitch of $L_{2\times3}$ intersection lineations. The observed pitch variation reflects superposition of the Alpine foliation across an already undulatory or folded S_2 fabric.

Importantly, close to the Alpine Fault, the data suggests a progressive increase in the NE pitch of the late Cenozoic mylonitic lineation in proximity to that structure. Between Franz Josef and Fox Glaciers, the mylonitic stretching lineation varies dramatically in its NE pitch over a range of 70° from ~20 to 90° (Fig. 14). Our data suggests that the more steeply pitching of these stretching lineations tend to occur in close proximity to the Alpine Fault. This lineation pattern will be discussed further below.

7. Discussion

7.1. Processes accommodating crustal-scale ramping and oblique convergence

G.P.S.-derived geodetic data indicate that the surface of the Southern Alps deforms transpressively at an observation scale of ~10–20 km. Particle velocities relative to the Australian Plate remain approximately parallel to the plate motion vector, ~20° to the strike of the Alpine Fault, while decelerating across a >100-km-wide region of active surface faulting to the east of the Main Divide (Beavan et al., 1999). Geodetically this deformation is expressed by a 4–5 mm/year reduction (Δv) in convergent velocity (V_t) across the width of this outboard zone (Fig. 15a). The plane geodetic deformation is dilatational (area is reduced) and displacement gradients parallel to the Alpine Fault are much smaller than those transverse to it (Beavan et al., 1999). If representative of flow at depth (Bourne et al., 1998), the velocity field implies that middle crustal rocks are undergoing a transpressive crustal thickening as they move west across the wide deforming zone to the east of the Alpine Fault (Fig. 15b, region 1). Progressive crustal thickening is supported by seismic reflection data showing a westward deepening in the reflection Moho from ~25 to 45 km across the central part of New Zealand's South Island (Fig. 2b). Transpression thus affects Pacific Plate rocks during an early phase of their westward transport, prior to their interaction with the Alpine Fault ramp. Ductile fabrics forming in a wrench-style transpression zone involving down-dip extension are predicted to have oblate strain fabrics and a down-dip direction of maximum finite extension (Sanderson and Marchini, 1984; Tikoff and Fossen, 1999), features that accord with our observations of the non-mylonitic Alpine Schist. For a convergence angle of ~20°, as in central South Island, the finite extension direction would be established in a down-dip direction after only a small amount of accumulated deformation. This relationship reflects the efficiency with which the irrotational vertical stretching increments are superimposed (e.g. Tikoff and Fossen, 1999), and can explain the down-dip plunge of mineral lineations in the Alpine Schist.

Eventually middle crustal rocks on the Pacific Plate encounter the Alpine Fault ramp (Fig. 15a). There, ~30–50 km to the east of the surface trace of the Alpine Fault, a late Cenozoic phase of ramp-related deformation must take place. The nature and intensity of this deformation will depend on ramp angle (θ_1), the mechanism(s) of differential uplift or tilting, and the distribution of strength and curvature along the ramp (e.g. Sanderson, 1982; Knipe, 1985). 'Pro-step up' shears in the finite element models of Beaumont et al. (1996) and Waschbusch et al. (1998) are similarly antithetic, accommodating a rotation of incoming crust against the relatively rigid and cold crystalline footwall of the Alpine Fault. Shears in the above-cited 2D models are not vertical, but become nearly so if 3D wrenching (strike-slip) is introduced into the modelling (e.g. Braun and Beaumont, 1995). Another possible mode of hanging wall bending, not mutually exclusive of shear failure, is pure bending or flexure (Fig. 15c) (e.g. Buck, 1988; Axen and Bartley, 1997). In the latter mechanism the distribution and width of strain depends on the radius of curvature and flexural rigidity of the crust. The flexed crust may behave as

a failed single beam or as a series of mechanical layers, each of which is undergoing flexural-slip and bending internally (e.g. Erickson and Jamison, 1995; Erickson et al., 2001). According to Erickson et al. (2001), in a 2D (thrust) situation, serial failure on steeply dipping backshears is favoured over pure bending or flexure where the ramp angle is sharp, and the effective basal friction is low. In the former case, the spacing between the backshears is probably controlled by crustal strength (narrower where weaker), strain-softening in the rock (softening favours larger spacing) and the mean normal stress (spacing decreases and shears coalesce with increasing depth into the ductile zone (Erickson et al., 2001).

Our field data indicate that a near-vertical backshearing mode of ramp deformation in the central part of the Southern Alps near Franz Josef Glacier has been an important process accommodating tilting and uplift of delaminated Pacific Plate rocks onto the oblique ramp of the Alpine Fault (Fig 15b, region 2). The data includes the occurrence of: (1) closely (~0.5 m) spaced, near vertical shears in the exhumed late Cenozoic brittle-ductile transition zone that strike subparallel to the Alpine Fault, and have an antithetic sense of dip-slip relative to that fault, and (2) a pervasive top-down-to-the east sense of late-stage ductile shear in the lower ~7 km, nonmylonitic part of the Alpine Fault's hanging wall (Little et al., 2002). The remarkably systematic spacing and attitude of the latter structures support an escalator-like, backshearing model of hanging wall deformation, as is Cox and Findlay's (1995) recognition of east-verging brittle faults of late Cenozoic age near the Main Divide of the Southern Alps (Fig. 15a). Also, the persistently near-vertical attitude of foliations on both sides of the ramp is consistent with vertical shear but not flexural-slip or bending (Fig. 15a). If the latter was important, preexisting vertical foliations to the east would have been rotated to moderate NW dips above the ramp. For simplicity, we show the ramp as an abrupt boundary, whereas in nature it is more likely to evolve into a curved shape (e.g. Strayer and Hudleston, 1997), as is implied by downward shallowing in dip of Alpine Fault reflectors (Fig. 2b). For a mean Alpine Fault dip of ~45°, vertical shear would structurally attenuate originally horizontal layers in the incoming crust by 25%, as is consistent with thermobarometric data, which indicates that the isograd sequence has been thinned (Grapes and Watanabe, 1992).

Vertical backshears are apparently absent ~30 km to the north of Franz Josef Glacier near Whataroa River and seem to be restricted in their distribution to a central part of the Southern Alps (Fig. 2). This style of supra-ramp deformation has been recognised only in the central zone of highest uplift rates, deepest exhumation, and narrowest orogenic width in the Southern Alps. There, a relatively sharp ramp angle may characterise the Alpine Fault at depth. Also, the combination of high heat flow (Koons, 1987; Craw, 1997) and near-lithostatic pore fluid pressures (Stern et al., 2001) mean that the Alpine Fault's hanging wall in this central Alpine region is likely to have a low flexural rigidity. Together, these factors may account for its failure by vertical shear style of ramp deformation rather than its bending into a longer wavelength flexure (e.g. Axen and Bartley, 1997; Erickson et al., 2001). The latter style may characterise wider parts of the orogen to the north and south.

Dextral-oblique shear directions at Franz Josef Glacier indicate that some strike-slip is partitioned into the Alpine Fault's hanging wall. If the vertical shears at Franz Josef Glacier acted solely to accommodate local differential uplift and tilting across the ramp, then they would have a down-dip shear direction (e.g. Apotria et al., 1992). Another kinematic role that vertical shears may have in regions of oblique motion is to partition some of the strike-slip component into the hanging wall of the main fault. In the latter case, the shears would not necessarily accommodate any differential uplift, and are predicted to have horizontal to NE pitching slip lineations (e.g. Jiang et al., 2001). Near Franz Josef Glacier, brittle-ductile shears striking parallel to the Alpine Fault are antithetic to the main fault in their sense of throw, suggesting differential uplift across a ramp, but also include a dextral-slip component, indicating some slip-partitioning behaviour. For this reason shear in the non-mylonitic part of the Alpine Schist (relative to the SE-dipping mean foliation) is dextral-normal, pitching SW, whereas that in the mylonite zone and on the Alpine Fault is dextral-reverse, pitching NE (Fig. 12a).

A final increment of late Cenozoic ductile deformation is acquired by rocks during their translation up the Alpine Fault ramp until such time as they pass through the contemporary brittle-ductile transition zone. Structural data indicates that ductile deformation is focused into the narrow Alpine mylonite zone, but with distributed shear extending several kilometres into the overlying rocks (Fig. 15b, region 3). If true, uplift rates should be relatively uniform to the east of the zone of distributed shear, a testable hypothesis in principal.

7.2. Transpressive flow in the Alpine Schist?

Is transpression a necessary consequence of oblique collision? Where has this type of ductile flow taken place in the deformation path of the Alpine Schist? Documenting rotation of differently oriented elongate biotite laths in 2D, Holcombe and Little (2001) showed that a garnet zone schist near Franz Josef Glacier had accumulated a zone-thinning type of general shear deformation. The pattern of rotation of the laths implied a down-to-the-east shear strain of ~0.6 together with a significant irrotational thinning of the schists. The inferred sectional kinematic vorticity in a vertical plane parallel to foliation dip was ~0.2, indicating a significant 'pure shear' component to the deformation since growth of the biotites. The oblate shape of finite and incremental strain in the Alpine Schist and vertical elongation directions (biotite, hornblende mineral lineations) imply that this irrotational component involved a maximum

finite extension that was down-dip. By themselves, fabric observations cannot identify where or when a finite transpression took place, if the shear component accrued at the same time as the 'pure shear', or if the deformation was a steady-state flow. In our view, the latter situation seems an unlikely possibility for the Alpine Schist.

The ductile shear direction that we measured in distal mylonitic rocks contradicts Walcott's (1998) model of vertical extrusion immediately to the east of the Alpine Fault, but is consistent with the kinematic model of Fig. 15a. By using the intersection normal of S/C' fabrics rather than stretching lineations to determine a shear direction, we have been able to avoid assumptions about the relationship of the shear direction to finite strain axes. Ductile shear bands in distal mylonitic rocks at Tatare Stream indicate that Pacific Plate rocks at depth were translated obliquely up the Alpine Fault parallel to the plate motion vector. A similar relationship in the brittle crust is recorded by fault-surface striations (Norris and Cooper, 1995, 1997). If regions 2 and 3 were being extruded up-dip by a transpressional deformation (Walcott's (1998) model), then the shear direction on the Alpine Fault would trend clockwise (down-dip) of the plate motion (e.g. Dutton, 1997). Vertical shearing at the base of the oblique ramp, however, will not change the transport direction on the fault (Apotria et al., 1992), even if transpression is taking place farther to the east (Fig. 15a).

To the east of the Main Divide and across the outboard ~100 km of the Southern Alps, active reverse faulting, westward deepening of the Moho, and the oblique trend of geodetic velocities imply a crustal-scale deformation that combines crustal thickening with distributed strike-slip (Norris et al., 1990; Beavan et al., 1999). We argue, therefore, that the observed transpressive flow in Alpine Schist probably took place when it resided in the middle crust of this 'outboard' part of the orogen. It is unclear to us to what degree the fabric record of such transpression has been removed by the later phases of exhumation-related deformation or to what degree some inherited (pre-late Cenozoic) imprints may still be retained in the fabric of the Alpine Schist.

The steep and variable pitch of mylonitic stretching lineations suggests that transpressive flow takes place locally in the Alpine mylonite zone at a distance of <1 km from the Alpine Fault. Jiang et al. (2001) interpreted variable, in part steeply plunging stretching lineations in the Alpine mylonite zone (Sibson et al., 1981), as evidence for oblique-slip transpression involving an irrotational component of down-dip stretch. According to their interpretation, variation in lineation pitch reflects variations in the ratio of simple to 'pure' shear. The slip direction we calculated in Tatare Stream is less steep than many stretching lineations in the central Southern Alps, supporting a triclinic flow model for the Alpine mylonite zone. Other supporting evidence includes the typical indistinctness of these stretching lineations, which implies an oblate shape of finite strain, and the conjugate disposition of oblique shear bands in mylonitic rocks, which indicates extension parallel to the Alpine Fault. The steepening in mylonitic lineation pitch that we have observed in proximity to the Alpine Fault (Fig. 14) implies that irrotational down-dip stretch may increase relative to simple shear within a few hundred metres of the Alpine Fault. Despite this local effect, the mylonitic shear direction remains approximately parallel to plate motion, ruling out ductile 'extrusion' of lower crust as a significant process overall.

Finite elongation lineations in the same rocks pitch SW moderately to steeply or are approximately down-dip. Discordance between shear vectors and finite elongation directions can arise in an oblique-slip transpression zones where the rocks undergo locally variable amounts of 'pure shear', for example parallel to the zone's dip (e.g. Jiang and Williams, 1998). We do not favour this model because of the Alpine Fault's slip direction relative to the plate motion vector. Instead, a non-steady state deformation sequence could generate the observed pattern of elongation lineations. If down-dip elongations initially developed in the transpression zone east of the Alpine Fault (region 1, Fig. 15b), then later dextral-normal shear at the base of the Alpine Fault ramp (region 2) could rotate the incremental and finite extension directions to a SW plunge. Quartz grain-shape fabrics in deformed veins are the closest thing we have to late-incremental strain markers, and these plunge SW in apparent agreement with this idea (Little, unpub. data).

7.3. 'Soft footprint' of late Cenozoic strain in the Alpine Schist

The Alpine foliation (S_3) is a steeply dipping composite fabric that in part predates the late Cenozoic oblique convergence and unroofing (D_4). Our minimum estimate of total ($D_3 + D_4$) shortening transverse to this Alpine foliation (50–75%) is indistinguishable from that of Holm et al. (1989), who measured shortening of quartz veins at Franz Josef Glacier. These authors suggested that the deformed veins were at least 2–10 Ma in age. We have shown, however, that shortening of this magnitude has accumulated since growth of the peak metamorphic porphyroblasts, ilmenite and garnet. The implications of our data are that the buckled quartz veins were probably emplaced prior to the late Cenozoic, and that late Cenozoic (D_4) contribution to ductile strain in this oblique collision zone must be less than 50–75%. Several post-biotite measures of strain indicate 30–40% of foliation-orthogonal shortening, an increment that we attribute to the late Cenozoic overprint. Biotite ^{40}Ar–^{39}Ar and K/Ar ages in the Franz Josef Glacier–Whataroa River regions are ~1–2 Ma (Batt et al., 2000); however, most workers interpret these as cooling rather than growth ages of the biotite. Our estimate of late Cenozoic incremental shortening is thus an interpretation, not a conclusion.

A late Cenozoic foliation-orthogonal shortening of

30–40% is consistent with the kinematic model in Fig. 15. For example, in the vertical plane parallel to the dip of the Alpine Fault (Fig. 15a), the model predicts 2D shortening strain perpendicular to the Alpine foliation plane of 27% if the foliation is a passively reinforced material plane and 32% if it tracks the finite flattening plane; maximum shortening values in three-dimensions are only slightly larger (Little, unpub data). To the first order, the inferred late Cenozoic strain magnitudes in the Alpine Schist agree with this model.

Despite ~90 km of crustal shortening in the Southern Alps during the past ~6.4 Ma (Walcott, 1998), the magnitude of ductile strain in the oblique collision zone is interpreted to be modest. That inherited fabric elements of probable Mesozoic age are widely preserved outside of the mylonite zone supports this inference. The reason for the late Cenozoic deformation having a 'soft footprint' is that oblique collision in the Southern Alps is dominated by rigid translation and erosion. Rocks migrate rapidly through the deforming zone, so they do not accumulate large finite strains. This is especially true of rocks currently at the surface, as these would have resided in the zone of oblique crustal thickening (region 1, Fig. 15b) for only a few m.y. before being uplifted along the Alpine Fault. The thermally weakened Alpine Fault defines a major discontinuity along the rapidly eroding, western edge of this asymmetric orogen (Koons, 1990). Classical vertical transpression zones with fixed boundaries (Sanderson and Marchini, 1984) seem an unlikely mechanism for accommodating large magnitudes of oblique convergence between plates, because finite strains will become prohibitively high. Models for crustal convergence need to account for the two-sided nature of mountain ranges such as the Southern Alps. In the South Island of New Zealand slip on or near a single structure, the Alpine Fault, accommodates most of the plate motion. The intensity of ductile strain to the east of that fault is therefore modest.

8. Conclusions

S/C' fabrics in protomylonitic rocks near Franz Josef Glacier record a dextral-reverse bulk shear direction at depth, the azimuth of which is within error of the contemporary Pacific–Australia plate motion vector. Transpressive ductile 'extrusion' is not a significant process in the Alpine Fault's hanging wall in the central Southern Alps.

In the oblique collision zone to the east of the Alpine Fault, deformation is inferred to accumulate in several noncoaxial stages rather than as a steady-state flow.

Initially, Pacific Plate rocks are subject to dextral transpression associated with oblate fabrics and a vertical maximum finite extension. The crust progressively thickens as the rocks move westward across the outboard part of the Southern Alps above a middle crustal decollement.

When these delaminated rocks encounter the crustal-scale oblique ramp of the Alpine Fault, they undergo an escalator-like vertical backshearing, with a sense of dip-slip that is antithetic to the Alpine Fault. Discrete, brittle-ductile shears accommodate this deformation at high levels, and coalesce downwards into a zone of pervasive backshearing below the BDTZ. This oblique-slip shearing tilts and thins the incoming Pacific Plate crust onto the underlying Alpine Fault, and also takes up a component of dextral-slip. The dextral-normal ductile shear results in a late-incremental stretching direction in the Alpine Fault's hanging wall that pitches SW. We infer that this style of supra-ramp deformation occurs only in the most rapidly uplifting, central part of the Southern Alps, because the Alpine Fault has a relatively sharp ramp angle at depth in this region, and because high heat flow and near-lithostatic pore fluid pressures contribute to the hanging wall having a low flexural rigidity. Together, these factors may lead to failure of the Pacific Plate at the ramp by vertical backshearing rather than its bending into a longer wavelength flexure.

As the rocks translate up the Alpine Fault ramp, shear is concentrated into a several kilometre-wide zone bordering the fault. In a narrow (hundreds of metres wide) zone adjacent to the fault, the noncoincidence of mylonitic stretching lineations with the shear direction suggests the flow is transpressive with irrotational component of stretch that is steeply plunging.

Since peak metamorphism in the Alpine Schist, finite strain in the non-mylonitic hanging wall of the Alpine Fault has involved a (minimum) foliation-orthogonal shortening of ~75% and an oblate foliation-parallel extension of ~100%. Deformation post-dating younger generations of biotite involved ~30–40% shortening orthogonal to the foliation, a final ductile deformation increment that we attribute to the late Cenozoic. The modest amount of late Cenozoic strain in the Alpine Schist reflects the importance of translation and erosion in accommodating oblique convergence across this two-sided orogen. Rocks migrate rapidly through the deforming zone so large finite strains do not accumulate. Most of the interplate slip is concentrated by erosion into a single structure. Transpression may play a relatively minor role in oblique collision.

Acknowledgements

This work was funded by research grants from the Faculty of Science, Victoria University of Wellington. The paper has benefited from thoughtful reviews by Keith Klepeis and Simon Cox, and from the editorial suggestions of Richard Norris. Stuart Bush made the oriented thin-sections. Discussions with T. Stern, P. Molnar, R. Grapes, J.K. Vry, R.J. Norris, and R.I. Walcott were helpful. E. Palmer took the photograph of Fig. 11b and contributed data to Figs. 10 and 12. R. Wightman contributed data to Fig. 14.

References

Apotria, T.G., Sneddon, W.T., Spang, J.H., Wiltschko, D.V., 1992. Kinematic models of deformation at an oblique ramp. In: McClay, K.R. (Ed.). Thrust Tectonics. Chapman and Hall, London, pp. 141–154.

Axen, G.J., Bartley, J.M., 1997. Field tests of rolling hinges: existence, mechanical types, and implications for extensional tectonics. Journal of Geophysical Research 102 (B9), 20,515–20,537.

Batt, G.E., Kohn, B.P., Braun, J., McDougall, I., Ireland, T.R., 1999. New insight into the dynamic development of the Southern Alps, New Zealand from detailed thermochronological investigation of the Mataketake Range pegmatites. In: Ring, U., Brandon, M., Lister, G., Willet, S. (Eds.), Exhumation Processes: Normal Faulting, Ductile Flow, and Erosion, pp. 261–282. Geological Society of London Special Publication 154.

Batt, G.E., Braun, J., Kohn, B.P., McDougall, I., 2000. Thermochronological analysis of the dynamics of the Southern Alps, New Zealand. Geological Society of America Bulletin 112, 250–266.

Beaumont, C., Kamp, P.J.J., Hamilton, J., Fullsack, P., 1996. The continental collision zone, South Island, New Zealand: comparison of geodynamical models and observations. Journal of Geophysical Research 101, 3333–3359.

Beavan, J., Moore, M., Pearson, C., Henderson, M., Parsons, B., Blick, G., Bourne, S., England, P., Walcott, R.I., Darby, D., Hodgkinson, K., 1999. Crustal deformation during 1994–1998 due to oblique continental collision in the central Southern Alps, New Zealand, and implications for seismic potential of the Alpine Fault. Journal of Geophysical Research 104 (B11), 25,233–25,255.

Blenkinsop, T.G., Treloar, P.J., 1995. Geometry, classification and kinematics of S–C and S–C' fabrics in the Mushandike area, Zimbabwe. Journal of Structural Geology 17, 397–408.

Bourne, S.J., England, P.C., Parsons, B., 1998. The motion of crustal blocks driven by flow of the lower lithosphere and implications for slip rates of continental strike-slip faults. Nature 391, 655–659.

Braun, J., Beaumont, C., 1995. Three-dimensional numerical experiments of strain partitioning at oblique plate boundaries: Implications for contrasting tectonic styles in the southern Coast Ranges, California, and central South Island, New Zealand. Journal of Geophysical Research 100 (B9), 18,059–18,074.

Buck, W.R., 1988. Flexural rotation of normal faults. Tectonics 7, 959–973.

Bull, W.B., Cooper, A.F., 1986. Uplifted marine terraces along the Alpine Fault, New Zealand. Science 234, 1225–1228.

Cooper, A.F., Norris, R.J., 1994. Anatomy, structural evolution, and slip-rate of a plate-boundary thrust: the Alpine Fault at Gaunt Creek, Westland, New Zealand. Geological Society of America Bulletin 106, 627–633.

Cooper, A.F., Barriero, B.A., Kimbrough, D.L., Mattinson, J.M., 1987. Lamprophyre dike intrusion and the age of the Alpine Fault, New Zealand. Geology 15, 941–944.

Cox, S.C., Findlay, R.H., 1995. The Main Divide Fault Zone and its role in the formation of the Southern Alps. New Zealand Journal of Geology and Geophysics 38, 489–499.

Craw, D., 1997. Fluid inclusion evidence for geothermal structure beneath the Southern Alps, New Zealand. New Zealand Journal of Geology and Geophysics 40, 43–52.

Craw, D., Rattenbury, M.S., Johnstone, R.D., 1994. Structures within greenschist facies Alpine Schist, central Southern Alps, New Zealand. New Zealand Journal of Geology and Geophysics 37, 101–111.

Davey, F.J., Henyey, T., Holbrook, W.S., Okaya, D.A.S.T., Melhuish, A, Henrys, S., Anderson, H., Eberhart-Phillips, D., McEvilly, T., Urhammer, R., Wu, F., Jiracek, G.R., Wannamaker, P.E., Caldwell, G., Christensen, N., 1998. Preliminary results from a geophysical study across a modern continent–continent collisional plate boundary — The Southern Alps, New Zealand. Tectonophysics 288, 221–235.

DeMets, C., Gordon, R.G., Argus, D.F., Stein, S., 1994. Effect of recent revisions to the geomagnetic reversal time scale on estimates of current plate motions. Geophysical Research Letters 21, 2191–2194.

Dewey, J.F., Holdsworth, R.E., Strachan, R.A., 1998. Transpression and transtension zones. In: Holdsworth, R.E., Strachan, R.A., Dewey, J.F. (Eds.). Continental Transpressional and Transtensional Tectonics. pp. 1–14. Geological Society of London Special Publication 135.

Dutton, B.J., 1997. Finite strains in transpression zones with no boundary slip. Journal of Structural Geology 19, 1189–1200.

Erickson, S.G., Jamison, W.R., 1995. Viscous-plastic finite-element models of fault-bend folds. Journal of Structural Geology 17, 561–573.

Erickson, S.G., Strayer, L.M., Suppe, J., 2001. Initiation and reactivation of faults during movement over a thrust-fault ramp: numerical mechanical models. Journal of Structural Geology 23, 11–24.

Findlay, R.H., 1987. Structure and interpretation of the Alpine schists in Copeland and Cook River Valleys, South Island, New Zealand. New Zealand Journal of Geology and Geophysics 30, 117–138.

Grapes, R.H., 1995. Uplift and exhumation of Alpine schist, Southern Alps, New Zealand: thermobarometric constraints. New Zealand Journal of Geology and Geophysics 38, 525–533.

Grapes, R.H., Watanabe, T., 1992. Metamorphism and uplift of the Alpine schist in the Franz Josef Fox Glacier area of the Southern Alps, New Zealand. Journal of Metamorphic Geology 10, 171–180.

Grindley, G.W., 1963. Structure of the Alpine Schists of South Westland, Southern Alps, New Zealand. New Zealand Journal of Geology and Geophysics 6, 872–930.

Holcombe, R.J., Little, T.A., 2001. A sensitive vorticity gauge using rotated porphyroblasts, and its application to rocks adjacent to the Alpine Fault, New Zealand. Journal of Structural Geology 23, 979–990.

Holdsworth, R.E., Strachan, R.A., Dewey, J.F., 1998. Continental Transpressional and Transtensional Tectonics. Geological Society of London, London.

Holm, D.K., Norris, R.J., Craw, D., 1989. Brittle and ductile deformation in a zone of rapid uplift: Central Southern Alps, New Zealand. Tectonics 8, 153–168.

Ilg, B.R., Little, T.A., 1999. Kinematic partitioning of transpressional elements in the Alpine Fault mylonite, New Zealand. Geological Society of America Abstracts with Programs 31 (7), A110.

Ji, S., Zhao, P., Saruwatari, K., 1997. Fracturing of garnet crystals in anisotropic metamorphic rocks during uplift. Journal of Structural Geology 19, 603–620.

Jiang, D., Williams, P.F., 1998. High-strain zones: a unified model. Journal of Structural Geology 20, 1105–1120.

Jiang, D., Lin, S., Williams, P.F., 2001. Deformation path in high-strain zones, with reference to slip-partitioning in transpressional plate-boundary regions. Journal of Structural Geology 23, 991–1005.

Kleffman, S., Davey, F., Melhuish, A., Okaya, D., Stern, T., Team, S., 1998. Crustal structure in the central South Island, New Zealand, from the Lake Pukaki seismic experiment. New Zealand Journal of Geology and Geophysics 41, 39–49.

Knipe, R.J., 1985. Footwall geometry and the rheology of thrust sheets. Journal of Structural Geology 7, 1–10.

Koons, P.O., 1987. Some thermal and mechanical consequences of rapid uplift: An example from the Southern Alps, New Zealand. Earth and Planetary Science Letters 86, 307–319.

Koons, P.O., 1990. Two-sided orogen: collision and erosion from the sandbox to the Southern Alps of New Zealand. Geology 18, 679–682.

Koons, P.O., 1994. Three-dimensional critical wedges: tectonics and topography in oblique collisional orogens. Journal of Geophysical Research 99, 12,301–12,315.

Larson, K.M., Freymueller, J., Phillipsen, S., 1997. Global plate velocities from the Global Positioning System. Journal of Geophysical Research 102, 9961–9981.

Little, T.A., Holcombe, R.J., Ilg, B.R., 2002. Ductile fabrics in the zone of active oblique convergence near the Alpine Fault, New Zealand: identifying the neotectonic overprint. Journal of Structural Geology 24, 193–217.

Masuda, T., Kugimiya, Y., Aoshima, I., Hara, Y., Ikei, H., 1999. A

statistical approach to determination of a mineral lineation. Journal of Structural Geology 21, 467–471.

Molnar, P., Anderson, H.J., Audoine, E., Eberhart-Phillips, D., Gledhill, K.R., Klosko, E.R., McEvilly, T.V., Okaya, D., Savage, M.K., Stern, T., Wu, F.T., 1999. Continuous deformation versus faulting through the continental lithosphere of New Zealand. Science 286, 516–519.

Norris, R.J., Cooper, A.F., 1995. Origin of small-scale segmentation and transpressional thrusting along the Alpine Fault, New Zealand. Geological Society of America Bulletin 107, 231–240.

Norris, R.J., Cooper, A.F., 1997. Erosional control on the structural evolution of a transpressional thrust complex on the Alpine Fault, New Zealand. Journal of Structural Geology 19, 1323–1342.

Norris, R.J., Koons, P.O., Cooper, A.F., 1990. The obliquely convergent plate boundary in the South Island of New Zealand: Implications for ancient collision zones. Journal of Structural Geology 12, 715–726.

Palmer, E., 2000. Growth and deformation history of Alpine Schist garnets. Franz Josef Glacier, Westland, New Zealand. M.Sc thesis, Victoria University of Wellington.

Passchier, C.W., 1998. Monoclinic model shear zones. Journal of Structural Geology 20, 1121–1138.

Pearson, C.F., Beavan, J., Darby, D.J., Blick, G.H., Walcott, R., 1995. Strain distribution across the Australian–Pacific plate boundary in the central South Island, New Zealand from GPS and earlier terrestrial observations. Journal of Geophysical Research 100, 22,071–22,081.

Prior, D.J., 1993. Sub-critical fracture and associated retrogression of garnet during mylonitic deformation. Contributions to Mineralogy and Petrology 113, 545–556.

Ramsay, J.G., 1967. Folding and Fracturing of Rocks. McGraw-Hill, New York.

Sanderson, D.J., 1982. Models of strain variation in nappes and thrust sheets: a review. Tectonophysics 88, 201–233.

Sanderson, D.J., Marchini, R.D., 1984. Transpression. Journal of Structural Geology 6, 449–458.

Sibson, R.H., White, S.H., Atkinson, B.K., 1979. Fault rock distribution and structure within the Alpine Fault zone: a preliminary account. Royal Society of New Zealand Bulletin 18, 55–65.

Sibson, R.H., White, S.H., Atkinson, B.K., 1981. Structure and distribution of fault rocks in the Alpine Fault Zone, New Zealand. Geological Society of London Special Publication 9, 197–210.

Simpson, G.D., Cooper, A.F., Norris, R.J., Turnbull, I.M., 1994. Late Quaternary evolution of the Alpine Fault Zone at Paringa, South Westland, New Zealand. New Zealand Journal of Geology and Geophysics 37, 49–58.

Stern, T., Kleffman, S., Scherwath, M., Okaya, D., Bannister, S., 2001. Low seismic wave speeds and enhanced fluid pressure beneath the Southern Alps of New Zealand. Geology, in press.

Strayer, L.M., Hudleston, P.J., 1997. Numerical modeling of fold initiation at thrust ramps. Journal of Structural Geology 19, 551–566.

Sutherland, R., 1995. The Australia–Pacific boundary and Cenozoic plate motions in the SW Pacific: some constraints from Geosat data. Tectonics 14, 819–831.

Sutherland, R., Norris, R.J., 1995. Late Quaternary displacement rate, paleoseismicity, and geomorphic evolution of the Alpine Fault: evidence from Hokuri Creek, South Westland. New Zealand Journal of Geology and Geophysics 38, 419–430.

Talbot, C.J., 1970. The minimum strain ellipsoid using deformed quartz veins. Tectonophysics 9, 47–76.

Teyssier, C., Tikoff, B., Markley, M., 1995. Oblique plate motion and continental tectonics. Geology 23, 447–450.

Thurlow, C., 1999. Deformation and metamorphism of Alpine Schist, Kokatahi River, north-central Westland, New Zealand. B.Sc. (Hon) thesis, Victoria University of Wellington.

Tikoff, B., Fossen, H., 1993. Simultaneous pure and simple shear: the unifying deformation matrix. Tectonophysics 217, 267–283.

Tikoff, B., Fossen, H., 1999. Three-dimensional reference deformations and strain facies. Journal of Structural Geology 21, 1497–1512.

Walcott, R.I., 1979. Plate motions and shear strain rates in the vicinity of the Southern Alps. In: Walcott, R.I., Cresswell, M.M. (Eds.), The Origin of the Southern Alps, pp. 5–12. Royal Society of New Zealand Bulletin 18.

Walcott, R.I., 1998. Modes of oblique compression: Late Cenozoic tectonics of the South Island of New Zealand. Reviews of Geophysics 36, 1–26.

Wannamaker, P.E., Jiracek, G.R., Stodt, J.A., Caldwell, T.G., Gonzalez, V.M., McKnight, J.D., Porter, A.D., 2001. Fluid generation and pathways beneath an active compressional orogen, the New Zealand Southern Alps, inferred from magnetotelluric data. Geophysical Journal International, in press.

Waschbusch, P., Batt, G., Beaumont, C., 1998. Subduction zone retreat and recent tectonics of the South Island of New Zealand. Tectonics 17, 267–284.

Wellman, H.W., 1979. An uplift map for the South Island of New Zealand, and a model for the uplift of the Southern Alps. Royal Society of New Zealand Bulletin 18, 13–20.

Wightman, R., 2000. The fabrics and ductile microstructures in the Alpine Schist and mylonite zone near Fox Glacier, New Zealand. B.Sc. (Hon) thesis, Victoria University of Wellington.

Woodcock, N.H., 1986. The role of strike-slip fault systems at plate boundaries. Philosophical Transactions of the Royal Society of London, Series A 317, 13–29.